An Australian Government Initiative

Funded through the Murray–Darling Water and Environment Research Program

Australia's National Science Agency

MD-WERP Deliverable: T1.FS3

Assessing the sensitivity of water resources in the Murray-Darling to fire and climate change

David E. Robertson, Hongxing Zheng, Durga Lal Shrestha, Francis H.S. Chiew

August 2023

Citation

Robertson DE, Zheng H, Shrestha DL, Chiew FCHS (2023) Assessing the sensitivity of water resources in the Murray-Darling to fire and climate change. MD-WERP Deliverable T1.FS3, CSIRO, Australia.

Copyright

Important disclaimer

Contents

Figures

Acknowledgments

This work was undertaken as a part of the Murray-Darling Basin Water and Environment Research Program (MD-WERP) Climate Adaptation Theme. The MD-WERP is an Australian Government initiative to strengthen scientific knowledge of the Murray–Darling Basin that is managed through a partnership between the Murray–Darling Basin Authority (MDBA), Commonwealth Environmental Water Office (CEWO) and the Department of Climate Change, Energy, the Environment and Water (DCCEEW).

The authors pay respect to the Traditional Owners and their Nations of the Murray−Darling Basin. We acknowledge their deep cultural, social, environmental, spiritual and economic connection to their lands and waters.

Executive summary

Bushfires have traditionally been understood to have impacts on long-term water availability. Climate change is projected to increase the frequency and intensity of bushfires and therefore the effects of climate change on bushfires may be expected to amplify the direct impacts of climate change on catchment runoff. Many previous investigations have estimated the impacts of historical fires on catchment runoff, and the impacts of climate change on catchment runoff, but few have considered the interactions. In this study we have assessed the potential impacts of bushfires on water availability under a changing climate for more than 100 catchments in the Murray-Darling Basin. To assess the impact of bushfires on future water availability we established modelling methods that relate (i) climate data to fire weather, (ii) fire weather to the area of forest burnt and changes in leaf area index (LAI) due to bushfire, (iii) post-fire recovery of LAI, and finally, (iv) catchment runoff to LAI. We calibrate and demonstrate the performance of each of the models and examine their sensitivity to LAI changes. We then use the modelling chain to assess changes in catchment runoff characteristics resulting from a hotter and drier future climate, characterised by a 10% decline in rainfall and 2°C increase in temperature, relative to the historical climate, and compare these changes to those obtained using more traditional modelling methods that do not consider the effects of bushfires.

We find that our methods for predicting burnt forest areas from fire weather, changes in LAI due to fire and the recovery of LAI following fire represent historically observed data and provide robust quantification of prediction uncertainties. We also find that the performance of the adapted hydrological model that is responsive to LAI changes is equal to or slightly better than the unadapted model for out-of-sample runoff predictions. Across the catchments investigated, modelled runoff is most strongly sensitive to LAI in forested catchments, while many catchments show little sensitivity.

Under the investigated future climate scenario, we find that the fire weather is projected to be more severe, and frequency and extent of bushfires is projected to increase. Catchment average LAI is projected to decrease due to the increased frequency and extent of bushfires, but the reductions are relatively small because fires are still expected to occur relatively infrequently and any individual fire will only cover part of the catchment. Changes in future runoff are expected to be dominated by the direct impacts of changes in future rainfall and potential evaporation. Including the effects of bushfires in modelling the runoff response to climate change had little impact on mean annual runoff for the majority of catchments investigated, while for a small number of catchments reductions in mean annual runoff were smaller when the effects of bushfires were included in modelling. While modelled changes in mean annual runoff were generally insensitive to the effects of bushfires, high and low flow conditions were observed to be sensitive with smaller reductions in high flow conditions and larger reductions in low flow conditions when the effects of bushfires are represented in hydrological modelling. These results indicate that using traditional hydrological modelling that does not explicitly consider the effects of bushfires for climate change projections will provide robust estimates of changes in mean annual flow, however if future changes in daily streamflow characteristics are important for management, then the effects of bushfires may need to be modelled.

1 Introduction

Wildfires are well known to have significant impacts on the hydrological cycle (Boyer et al., 2022). Impacts of fire occur through long and short-term changes in vegetation cover and composition, mobilisation of sediments and other nutrients, modification of soil surface properties, including surface sealing, and, in cryospheric zones changes to the soil thermal properties and permafrost (Boyer et al., 2022; Li et al., 2021; Paul et al., 2022). These direct impacts of fire lead to changes in runoff volumes and rates, and the degradation of water quality in rivers and water storages all of which can pose challenges to the management of water resources.

In Australia, many investigations have sought to quantify the impacts of historical fires on the hydrological cycle. Early work on fire impacts in the Murrumbidgee catchment during the early 1970’s showed that in the years immediately following a fire, catchment runoff volumes and sediment concentrations tended to be much higher than what would be predicted from pre-fire rainfall and streamflow data (Brown, 1972). The effects of fire on both catchment runoff and sediment concentrations were observed to decrease with time.

In several Melbourne water supply catchments, and also those adjacent in the southern Murray-Darling Basin, Langford (1976) identified multi-decade reductions in runoff coefficients following large scale fires. Kuczera (1987) established an empirical relationship between catchment yield and forest age in the Melbourne water supply catchments using the Langford dataset. This relationship suggested that catchment runoff could decline by up to 50% in the first 20-30 years following a fire and take up to 150 years to recover to its pre-fire state. Numerous field experiments were undertaken to better understand the physical processes leading to the observed declines in catchment runoff. These studies found that streamflow declines are related to changes in evaporation as forests age, primarily related to changes in forest sapwood area and leaf area (Benyon et al., 2010; Vertessy et al., 2001).

Knowledge gained in the Mountain Ash (*Eucalyptus regnans)* and Alpine Ash (*Eucalyptus delegatensis*) forest-dominated Melbourne water supply catchments has been extrapolated to provide estimates of the impacts of historical fires on catchment water yields in south-east Australia and other regions. The magnitude of estimates of fire impacts have varied considerably. Initial estimates of the impacts of fires in alpine Victoria in 2003 and 2006-7 were that annual streamflow could reduce by up to 50% by the mid-2020s in some catchments (Hill et al., 2008; Mannik et al., 2013). Recent research found that in much of south-east Australia initial increases in runoff coefficients following fires are observable in streamflow time series, but subsequent longer-term declines, such as those adopted in the analysis of Hill et al. (2008) and Mannik et al. (2013), could not be confirmed (Khaledi et al., 2022). The findings of Khaledi et al. (2022) are more consistent with the results of field-based studies of the hydrological responses to fire in mixed-eucalypt species forests (e.g. Brown, 1972; Lane and Mackay, 2001) that have typically observed an initial increase in runoff following fire or forest management, but no long-term runoff declines.

The contrasting findings from investigations into the hydrological responses to fire can partly be attributed to differing responses of eucalyptus forests to fire. Mountain and Alpine Ash species are typically characterised as ‘seeders’ whereby trees tend to be killed when their leaves are scorched and the forest regenerates from seed (Gill, 1981). Other eucalyptus species, including Messmate (Eucalyptus obliqua) and narrow-leaved peppermint (Eucalyptus radiata), tend to be ‘sprouters’ that are less likely to be killed by a fire and forest regeneration occurs when existing trees regrow from protected buds, that can be above or below the ground surface (Gill, 1981). In addition to differences in forest phenological responses to fire, the severity of fires also impacts the immediate response and subsequent recovery of vegetation (Gill, 1981).

Forest regrowth characteristics have strong impacts on evaporation and consequently catchment runoff. Following fire, forests that are dominated by ‘seeders’ tend to rapidly establish stem densities, sapwood densities and a leaf area index that is much higher than a mature forest, which then declines as the forest ages through self-thinning (Benyon et al., 2023; Vertessy et al., 2001). This leads to evaporation rates falling immediately following a fire because of initial vegetation loss, then increasing to higher than pre-fire levels as the forest regenerates and subsequently declining as the forest matures. Hydrological models have generally represented evaporation changes during fire recovery by relationships between evaporation to leaf area index or canopy conductance and stand age (Benyon et al., 2023). Forests dominated by ‘sprouters’ have been less well studied, but are often assumed to follow the same characteristics (e.g. Hill et al., 2008; Mannik et al., 2013).

The parameterisation of LAI-age models has been historically limited by the need to substitute space for time in LAI and canopy conductance data, meaning that variations in LAI were characterised using spatially separated forest stands of different ages (Benyon et al., 2023). Assumptions have then been that species all follow the same LAI/age trajectory (i.e. there is no spatial variation in underlying forest LAI) and that initial fire or forest management impacts on LAI are consistent across the spatially separated forest stands. Therefore, while the general form of LAI-age relationships may be appropriate, their parameterisations may not account for spatial variations in underlying LAI and the initial impacts of fire on LAI, limiting their ability to be generalised for Basin-scale analysis. Remotely sensed time series of vegetation indices, such as LAI (e.g. Zhu et al., 2013), are now available and can potentially provide for more generalised analysis of LAI responses to fire and support better understanding of contrasting assessments of historical fire impacts in Murray-Darling Basin.

The frequency of severe fire weather conditions in Australia has been increasing in recent decades and with it the extent and frequency of wildfires (Canadell et al., 2021). Notably the greatest changes have been in south-eastern Australia and the headwater catchments of the Murray-Darling Basin. Climate change projections show increasing temperatures and changing rainfall patterns are expected to result in increasing fire weather severity (Dowdy, 2020) and as a result bushfire frequency, severity and potentially extent. Therefore, the future impacts of fire on water resources availability and management are expected to be amplified.

Chiew et al. (2008) undertook an assessment of the impacts of fire on mean annual runoff under a future climate across the Murray-Darling Basin, finding that fire would reduce future mean annual runoff by 1% in a small number of catchments and not at all in many others. Their assessment adapted the models developed by Hill et al. (2008) averaged over 100 years and considered changes in mean annual forest fire danger index. As such, the assessment provides only a first order evaluation of fire impacts on mean annual runoff that neglects inter-annual variability and non-linearities in climate change impacts on fire weather severity and fire impacts on vegetation and hydrological processes.

In this study we seek to provide insight into the likely sensitivity of water resources to climate change considering the effects of fire. We establish a hydrological modelling method that seeks to represent the impact of fire, and other changes in vegetation, on catchment runoff by relating evaporation to remotely sensed observations of LAI. We then develop an approach to generate future projections of LAI as impacted by fire. The approach uses models that (a) relates fire weather severity to fire occurrence and burnt areas, (b) relates fire weather severity to LAI impact due to fire occurrence, and (c) characterises the recovery of LAI in the years following a fire. Projections of future LAI and consistent climate data are used to force our hydrological model to generate projections of future runoff. The impacts of climate change on catchment runoff characteristics generated using our modelling approach are compared to those produced using a more traditional approach that neglects the impacts of fire. The next section describes the detailed methods adopted in our analysis. Results evaluating the modelling methods and summarising climate change projections are presented in Section 3. Section 4 discusses how the findings from the study relate to previous assessments and highlights the study limitations and future opportunities.

2 Methods

2.1 Approach and assumptions

To understand the sensitivity of water resources to the combined impacts of fire and direct climate change we establish a modelling chain that enables the projection of future change on the incidence and severity of fire and the impact of fire on catchment runoff.

We assume that the primary impact of fire on catchment runoff is by altering the vegetation characteristics of the catchment. We therefore establish a rainfall-runoff modelling approach that responds to changes in vegetation. We assume changes in vegetation at the catchment scale are best characterised by remotely sensed leaf area index (LAI) data, on the assumption that these adequately represent vegetation characteristics.

To develop future projections using our rainfall-runoff model we require projections of all forcing data, which includes climate forcing (rainfall and potential evaporation) and also LAI. We therefore develop methods to generate projections of catchment average LAI, as impacted by fire, from climate projections. Our approach to generating these catchment scale LAI projections creates models that describe the extent of future fires, their immediate impact on LAI and the post-fire recovery of LAI. These models can then be forced with future climate projections to assess the combined impact of direct climate change on fire and water availability.

We compare projections made using our rainfall-runoff modelling that considers the effects of fire to standard approaches to generating future runoff projections that use standard rainfall-runoff models.

In the remainder of this section, we firstly introduce the datasets used for the analysis, then describe the approaches taken to establish modelling and finally explain how the models have been used to generate projections of future runoff.

2.2 Data

2.2.1 Catchment data

We investigate 245 catchments in Victoria and New South Wales where high quality streamflow observations are available to calibrate hydrological models, including catchments that are outside the Murray-Darling Basin. The streamflow observations and catchment delineations are obtained from the Bureau of Meteorology's Hydrologic Reference Stations (Zhang et al., 2013, see http://www.bom.gov.au/water/hrs/about.shtml). Catchment scale forcing data for the models are derived by taking area-weighted averages of gridded data estimates used to support the Australian Water Outlook (Frost et al., 2018; Jones et al., 2009).

2.2.2 Bushfire extent maps

Bushfire extent maps are obtained for Victoria (https://discover.data.vic.gov.au/dataset/fire-history-records-of-fires-across-victoria1) and New South Wales (https://datasets.seed.nsw.gov.au/dataset/fire-history-wildfires-and-prescribed-burns-1e8b6). Raw datasets represent the extents for individual fires as polygons with attributes characterising fire type, fire season, burnt area and in many cases fire severity.

The Victorian and NSW datasets are firstly merged and then grids of annual fire extent at a 1 km spatial resolution are derived by rasterising all polygons for each fire season.

2.2.3 Leaf Area Index

Remotely-sensed LAI data generated using the Zhu et al. (2013) approach are used for this study (https://drive.google.com/drive/folders/0BwL88nwumpqYaFJmR2poS0d1ZDQ?resourcekey=0-9IRE9s-0tFGfwB5qTpLjZw). This global dataset is available at 0.083° spatial resolution at 15-day time steps for the period July 1981 to December 2016. Data are firstly resampled to match the 1 km spatial resolution of the fire extent data set. The 15-day LAI data are noisy, display seasonal patterns and at a higher temporal resolution than the fire extent data. To obtain an annual LAI time series we firstly apply a 12-month centred moving average filter, and then extract the annual minimum values for each fire year (year to June).

2.2.4 Forest Fire Danger Index

The Forest Fire Danger Index (McArthur, 1967; Noble et al., 1980) (FFDI) is used to characterise fire weather conditions. Data for initial analysis are obtained from (Dowdy, 2020), however we rederived these using gridded rainfall and temperature and relative humidity data from the Bureau of Meteorology (Jones et al., 2009) and ERA5 wind data (Hersbach et al., 2020) so that a consistent set of forcing could be used for historical simulations and future projections. Gridded daily FFDI is computed at a 5 km spatial resolution for the entire domain used for this analysis and then resampled to the 1 km spatial resolution of the fire extent data. Area-weighted catchment averaged FFDI is also computed for all 245 catchments.

Annual time series of fire weather indicators are obtained by counting the number of days above a threshold for spatial units, either grid cells or area-weighted catchment averages. Thresholds for computing the annual time series include the lower bounds for Very High (FFDI > 25), Severe (FFDI > 50) and Extreme (FFDI >75) fire danger formerly used in Victoria and adopted for national scale fire analysis (Canadell et al., 2021), and also the 90th percentile of the location specific historical distribution.

2.2.5 Land cover

Land cover data is obtained from the major vegetation groups layer of version 6.0 of the National Vegetation Information System (NVIS, https://www.dcceew.gov.au/environment/land/native-vegetation/national-vegetation-information-system). We assume that the present-day land cover data best represent the land cover during the entire period of analysis.

The NVIS land cover dataset integrates state mapping of the present-day vegetation coverage at a 100 m spatial resolution. Land cover is classified into 33 different vegetation groups, primarily based on the structural form of vegetation. Land cover data were upsampled to the 1 km spatial resolution of the bushfire extent maps by taking the class of the land cover grid cell nearest the centroid.

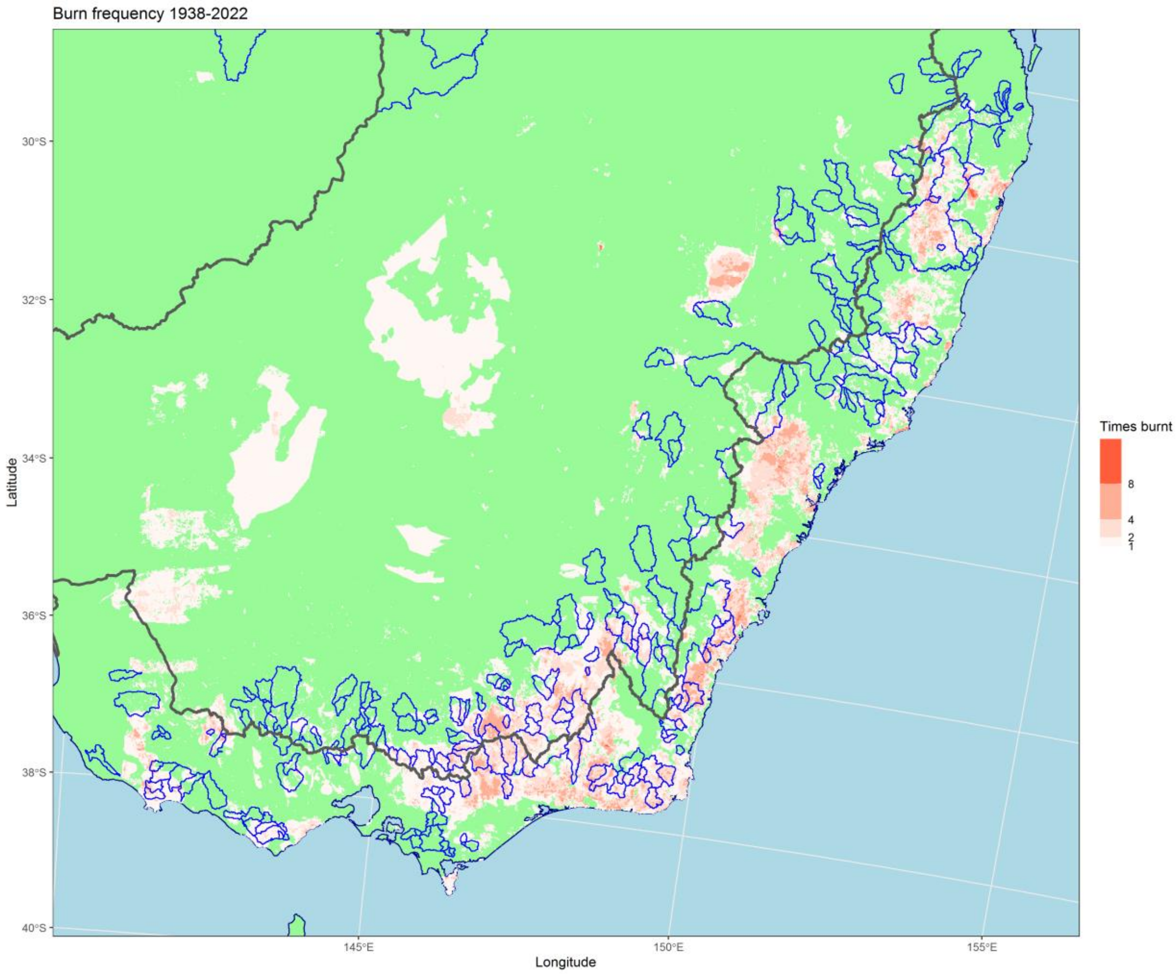

Figure 1 Geographic location of the 246 Bureau of Meteorology's Hydrologic Reference Stations (HRS) catchment boundaries (in blue), the Murray-Darling Basin (MDB, black). The background red colour ramp shows the frequency of fires for 1938–2022, with the green shading indicating non-burnt areas.

2.3 Modelling vegetation change on streamflow

2.3.1 Hydrological model conceptualisation

Current practice to investigate the impacts of climate change on catchment runoff in the Murray-Darling Basin (MDB) involves running future climate inputs through a calibrated conceptual model, such as GR4J (Perrin et al., 2003), with the same parameter values used to model runoff under both historical and future climates. We adopt this approach as a benchmark assessment of the impacts of climate change on catchment runoff (Charles et al., 2020; Chiew et al., 2017; Prosser et al., 2021).

To represent the effect of vegetation on catchment runoff we adapt the GR4J hydrological model (Figure 2) so that actual evaporation is related to LAI and the level of the production store (S) rather than only the level of the production store.

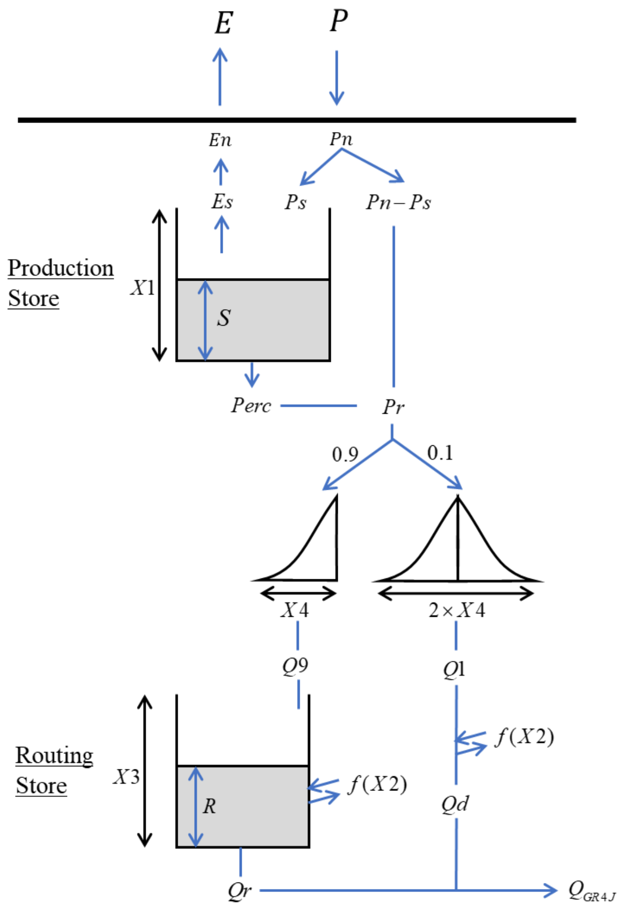

Figure 2 Schematic of the GR4J model.

In the original formulation of GR4J, the actual evaporation is given by

$$E_s = \frac{S\left(2-\frac{S}{x_1}\right) tanh\left(\frac{E_m}{x_1}\right)}{1+\left(1-\frac{S}{x_1}\right) tanh\left(\frac{E_m}{x_1}\right)}$$

Equation 1

where E_s is actual evaporation from the production store, $E_m = E_n$ is the net evaporation capacity and x_1 is the capacity of the production store.

We adapt the formulation of evaporation to include a dependence on LAI as follows,

$$E_m = E_n(a + b[1 - exp(-k \cdot LAI)])$$

Equation 2

where $\{a, b, k\}$ are parameters. In the published version of Equation 2, $a = 0.45$ and $b = 0.4$ and k is a calibrated parameter (Kondo, 1998; Sato et al., 2008). However, we modify this such that $b = (1 - a)$ and calibrate both a and k.

2.3.2 Model calibration

Hydrological models are calibrated to minimise an objective function using the Shuffled Complex Evolution algorithm (Duan et al., 1993). The selected objective function (Equation 3) has been commonly used to calibrate models for previous climate change impact assessments (Chiew et al., 2018; Viney et al., 2009). When calibrating the benchmark hydrological model only the four standard GR4J model parameters are optimised. However, when calibrating the extended model, an additional two parameters are required in the formulation of the evaporation response to LAI, so model calibration involves optimising six parameters.

$$OF = (1 - NSE) + 5(log(1 + bias))^{2.5}$$

Equation 3

where

$$NSE = 1 - \frac{\sum_{t=1}^{T}\left(Q_{s,t} - Q_{o,t}\right)^2}{\sum_{t=1}^{T}\left(Q_{o,t} - \bar{Q}_o\right)^2}$$

Equation 4

$$bias = \frac{(\bar{Q}_s - \bar{Q}_o)}{\bar{Q}_o}$$

Equation 5

and NSE is the Nash-Sutcliffe efficiency (Nash and Sutcliffe, 1970), $Q_{s,t}$ is the simulated streamflow for time step t ,$Q_{o,t}$ is the observed streamflow, $\bar{Q}_s$is the mean simulated streamflow, $\bar{Q}_o$is the mean observed streamflow and T the total number of time steps.

Models are calibrated to all available streamflow data between 1983 and 2018.

We assess the out-of-sample performance of the calibrated models using windowed cross-validation strategy. For each year in the historical record, we calibrate the hydrological model to all streamflow observations excluding the year of interest and subsequent year. We then generate simulations for the year of interest. The streamflow simulations for each year are then combined to form a single time series that is compared to observed streamflow using the NSE and $bias$ as measures of performance.

2.4 Relationship between fire weather and fire occurrence

For each catchment, we compute the forest area burnt in each year from using the bushfire extent maps and catchment boundaries. We explore the relationship between annual FFDI exceedance counts and (i) the probability of fire occurring in any catchment, and (ii) the area of forest burnt in each catchment.

We establish a statistical model, specifically the Bayesian Joint Probability modelling (BJP) approach (Wang and Robertson, 2011; Wang et al., 2009) using data for all catchments to relate the annual FFDI exceedance counts to forest burnt area. The BJP firstly applies a transformation to normalise and stabilise the variance of predictor and predictand data. It then assumes the transformed predictor and predictand data follow a censored multivariate normal distribution.

The use of data censoring allows the zero-valued observations in both the predictor and predictand data to be handled using the assumed continuous multi-variate normal distribution. Data censoring assumes that zero values are less than or equal to zero with an unknown precise value.

For this study, a log-sinh transformation is applied to normalise both the annual FFDI exceedance counts and the forest burnt areas in each catchment.

For known values of the predictor, annual FFDI exceedance counts, the distribution of forest burnt area for a catchment can be estimated by (a) conditioning the inferred multi-variate normal distribution of the transformed predictor values, (b) sampling from the conditional distribution, and (c) back transforming the sampled values using the transformation appropriate for the predictand (forest burnt area). In this way, stochastic realisations of forest burnt area can be generated from FFDI time series.

We evaluate the model predicting forest burnt area from FFDI exceedance counts and assess its performance using measures of bias and the statistical reliability of prediction uncertainty estimates.

2.5 Impact of fire on vegetation

To assess the impact of fire on vegetation we investigate the changes in remotely-sensed LAI that occur due to fire, including how these are impacted by fire weather, and also the recovery of LAI following a fire.

2.5.1 Leaf area index change due to fire

We examine the impact of fire on LAI by firstly computing the annual change in LAI for individual grid cells. Annual changes in grid cell LAI are then analysed by examining the distribution of changes conditioned on the occurrence of fire and the annual FFDI exceedance counts. The Annual FFDI exceedance counts are used rather than other measures of fire weather severity as it was found to be the best indicator to describe the occurrence of fire. Based on exploratory analysis we use a piece-wise linear regression to model the relationship between annual LAI change and annual FFDI exceedance counts.

$$\Delta LAI_{fire,s} = f\left(d_{FFDI>q90,s}\right) + \epsilon$$

Equation 6

where for location s, $\Delta LAI_{fire,s} = LAI_{-1,s} - LAI_{0,s}$, $LAI_{-1,s}$ is the LAI at the start of the year a fire occurred, $LAI_{0,s}$ is the LAI at the end of the year a fire occurred and $d_{FFDI>q90,s}$ is the annual FFDI exceedance counts, i.e. days above the site or catchment 90th percentile FFDI, and $\varepsilon \sim N(0, \sigma^2)$.

2.5.2 Post-fire recovery of leaf area index

The recovery of LAI following a fire is complex and has previously been found to be related to the initial fire impact and time since fire occurrence. For each grid cell we generated timeseries of LAI recovery after fire using the following:

$$Recovery_{t,s} = \frac{LAI_{t,s} - LAI_{0,s}}{LAI_{-1,s} - LAI_{0,s}}$$

Equation 7

where $LAI_{t,s}$ is the LAI t years after a fire, $LAI_{-1,s}$ is the LAI at the start of the year a fire occurred, $LAI_{0,s}$ is the LAI at the end of the year a fire occurred.

We initially graphically explored the relationship between the LAI recovery index and the number of years since fire and its variation with vegetation classes.

Many models have been used to describe LAI (Vertessy et al., 2001) and bushfire fuel accumulation (Gould and Gomes Da Cruz, 2012) as a function of time since fire, or forest stand age. Many of these models take the generic form whereby the LAI at some time after fire is the sum of exponential functions of stand age,

$$Recovery_t = \alpha + \sum_i \beta_i \, exp(-k_i t)$$

Equation 8

where t is the number of years after a fire and α, β_i and k_i are model parameters. The implementation of these models has either tended to be site specific, or parameterised such that the long-term, or steady state, LAI and initial fire impact on LAI are assumed uniform in space and time. These assumptions have been made due to the limited field observations of LAI that have been historically available. Our initial analysis of LAI data suggests considerable spatial variation in the average LAI values and that the impacts of fire on LAI also vary in space and with fire characteristics. Therefore, to account for these considerations and reduce the number of parameters required to model the recovery of LAI following fire, we adapted the generic formulations to make use of the time series of LAI, as follows

$$LAI_{t,s} = LAI_{-1,s} - \Delta LAI_{fire,s} exp(-kt^{\gamma}) + \varepsilon$$

Equation 9

where t is the number of years after a fire, s is a location identifier, $\Delta LAI_{fire,s} = LAI_{-1,s} - LAI_{0,s}$ and $\varepsilon \sim N(0, \sigma^2)$.

We estimate model parameters $\{k, \gamma, \sigma\}$ using a maximum likelihood approach for all forecast grid cells in the study region.

2.6 Assessing runoff sensitivity to fire under a future climate

We adopt a sensitivity approach to investigate the impact of fires on runoff under a future climate. We establish a single future climate scenario that is characterised by a 10% reduction in rainfall and a 2°C increase in temperature, and compare runoff projections to historical runoff simulations generated using historical observations of forcing data. For much of the Murray-Darling Basin this future climate scenario adopted represents approximately the median change in temperature projected by the CMIP6 global climate models and larger decreases in rainfall projected by approximately 25% of GCMs for the year 2065. To generate the projections, we simply multiply the historically observed daily rainfall by 0.9 and add 2°C to historical daily temperature observations.

Our modelling methods also require projections of windspeed, relative humidity, and potential evaporation. We assume that windspeed and relative humidity are unchanged while potential evaporation increases by 7%, which is consistent with other assumed changes (i.e. 2°C temperature increase and no change in relative humidity).

To generate projections of runoff we firstly create projections of daily FFDI for each catchment from the projected climate data. Using these projections, we compute the number of days the projected FFDI exceeds the historically observed 90th percentile FFDI value in each year to produce projections of annual FFDI exceedance counts.

Projections of forest burnt area are then generated using the modelled relationship between annual FFDI exceedance counts and forest fire burnt areas. As this relationship is uncertain, we use the statistical model to generate 1000 realisations of forest burnt area for each year. Where the projected forest burnt area exceeds the area of forest in a catchment, the projected forest burnt area is reset to the catchment's forest area.

Projections of catchment average LAI are then generated in multiple stages for each of the 1000 realisations of forest burnt area. We model only the effects of fire on LAI for the forested areas of each catchment and assume that the non-forested areas have the same LAI as historically observed. The changes in LAI due to fire impacts and recovery in the forested catchment areas are modelled at the 1km grid cells used in model development. The LAI for each forested grid cell is modelled as a time series, keeping track of the multiple variables required to estimate LAI, specifically $\Delta LAI_{fire,s}$, $LAI_{-1,s}$, and t. In our analysis we treat each grid cell in a catchment independently, thus disregarding the spatial arrangement of grid cells in computing catchment average LAI.

Each modelled forest grid cell is initialised with the LAI and time since fire corresponding to the start of the historical time series (1982).

For each year the projected burnt forest area is randomly distributed across the forest grid cells, consistent with our treatment of grid cells as being independent.

Where a grid cell is designated to be burnt in a given year,

a) the change in LAI for that year ($\Delta LAI_{fire,s}$) is estimated from Equation 6 using the projected FFDI exceedance count for the year, including taking a single sample from the residual distribution,
b) the LAI for that year is computed as $LAI_{-1,s} + \Delta LAI_{fire,s}$
c) the time since fire reset (i.e. $t = 0$),
d) the prefire LAI ($LAI_{-1,s}$) is updated to equal the LAI for the preceding year,

Where a grid cell is not designated to be burnt in a given year,

a) $\Delta LAI_{fire,s}$ and $LAI_{-1,s}$ are set to the previous year's values,
b) time since fire incremented by a year (i.e. $t = t + 1$),
c) the LAI is estimated using Equation 9, also taking a single sample from the residual distribution.

The catchment average LAI for each year is then computed by averaging across all forested and non-forested grid cells.

The 1000 time series of projected catchment average LAI, together with the single time series of projected rainfall and potential evaporation, are used to force the hydrological model to generate 1000 time series of projected runoff.

In addition to generating projections of future runoff, we also force our modelling workflow with historical climate forcing to product a 1000-member ensemble of historical runoff simulations.

We analyse the ensemble simulations for each catchment by firstly computing runoff statistics (mean, 5^{th} percentile, 95^{th} percentile and number of days below the simulated historical median) for each year and ensemble member. We then derive an ensemble of mean annual statistics by computing the mean runoff statistics over all years for each ensemble member. We summarise the ensemble of mean annual statistics using the ensemble mean, median, 5^{th} and 95^{th} percentiles. Finally, we compare projected with historical runoff by computing differences between these summary statistics.

3 Results

3.1 Hydrological modelling

3.1.1 Cross-validation performance

The GR4J model that is forced by LAI shows an out-of-sample NSE that is greater than or equal to that of the GR4J model that is not forced by LAI (Figure 3) for all but one catchment. In general, the improvements to the NSE tend to be small, but there are several cases where NSE improves by more than 0.1. Catchments where the out-of-sample NSE increases when using LAI as forcing tend to be clustered in headwaters of the Murrumbidgee catchment (Figure 4) but also occur in some of the drier regions of NSW. The out-of-sample biases tend to be small (less than 10%) for all catchments. In general, the GR4J model forced by LAI shows slightly higher biases than the model that does not use LAI forcing, however there are several catchments where the biases reduce. Catchments where the out-of-sample bias reduces when using LAI as forcing tend to be clustered in the high runoff-catchments in the south-east of the MDB (Figure 4).

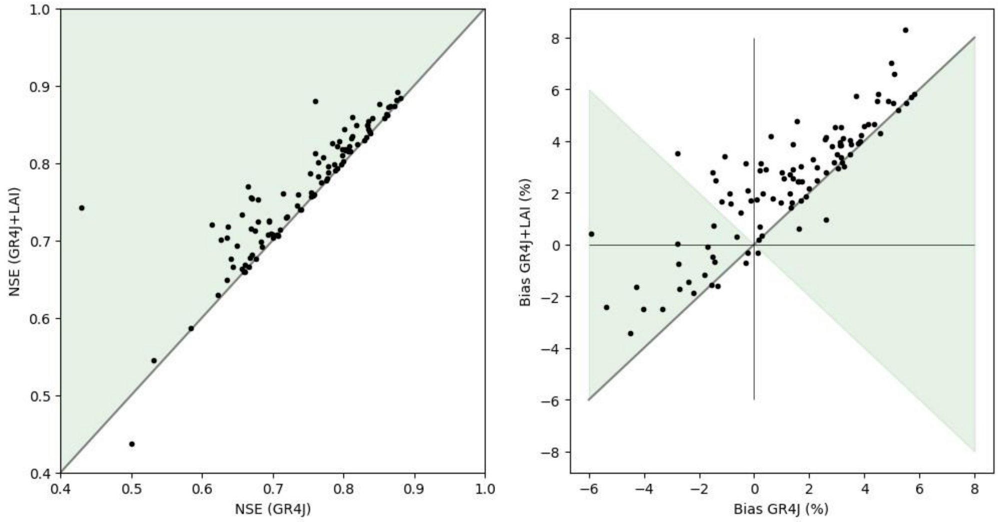

Figure 3 Comparison of cross-validation NSE and bias of standard and LAI-forced versions of GR4J hydrological model for the 104 catchments in the MDB where fire has been historically observed. Green shading indicates areas where LAI-forced version produces better cross-validation performance than the standard version.

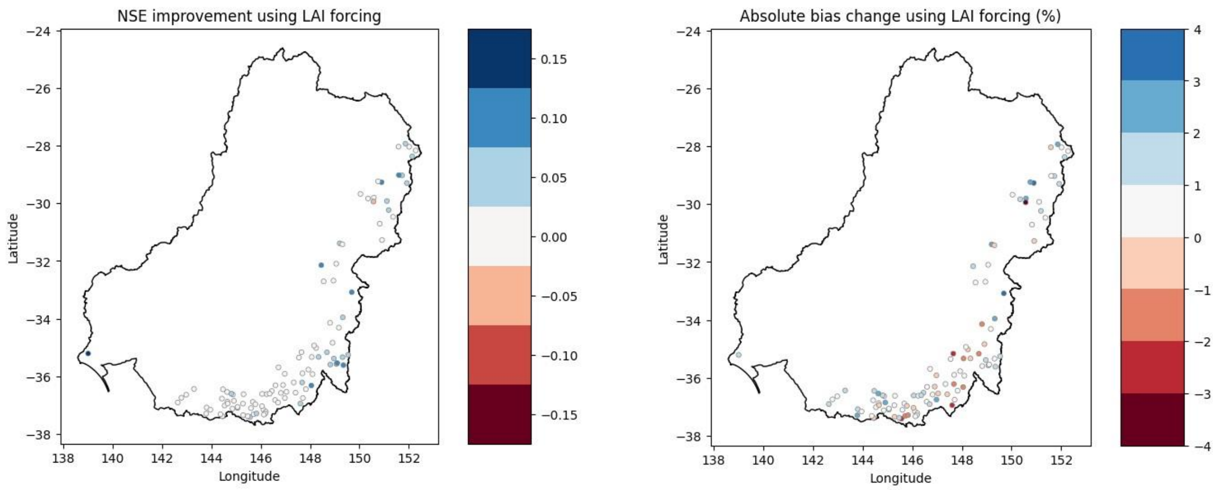

Figure 4 Spatial distribution of increases in NSE (left panel) and changes in absolute percentage bias (right panel) when LAI is used as a forcing in the GR4J hydrological model.

3.1.2 Sensitivity of simulations to leaf area index

Following calibration, the GR4J model forced by LAI shows a range of sensitivities to varying LAI between the Hydrologic Reference Station (HRS) catchments (Figure 5). Figure 5 illustrates flow-duration curves for daily, monthly and annual runoff generated by models forced by the observed LAI time series, and climatology (monthly mean) LAI time series and time series generated using the maximum and minimum values in the observed LAI record for three example catchments. Calibrated models for some catchments (e.g. 412050) show no sensitivity to LAI, which can be because there is little variation in the LAI timeseries or that changes in LAI have little impact on catchment evaporation. The latter may be the result of other factors, such as limitations on soil moisture from low rainfall having a stronger influence on catchment-scale evaporation than vegetation changes. However, runoff predictions from calibrated models for other catchments (e.g. 410057 and 405209) can be strongly responsive to LAI variations at daily, monthly and annual time scales (Figure 5). For both the sensitive catchments, differences between the flow-duration curves generated using the observed and climatology LAI time series are very similar, particularly for the daily and monthly data. Some differences between the flow-duration curves generated using observed and climatology LAI become apparent for annual data, however the differences are relatively small and the two curves closely follow one another over the entire range of flows. The flow duration curves generated using the maximum and minimum LAI values depart significantly from those generated using the observed LAI time series. Simulated runoff generated using the minimum LAI as forcing data is significantly higher, almost double in the case of annual data, than simulations generated using the observed LAI. Conversely, runoff simulations generating using the maximum LAI as forcing data are consistently lower than those generated using observed LAI forcing. This behaviour is expected by the relationship relating LAI to catchment potential evaporation (Equation 2), where increasing LAI leads to increase catchment evaporation and hence water available for runoff will decline.

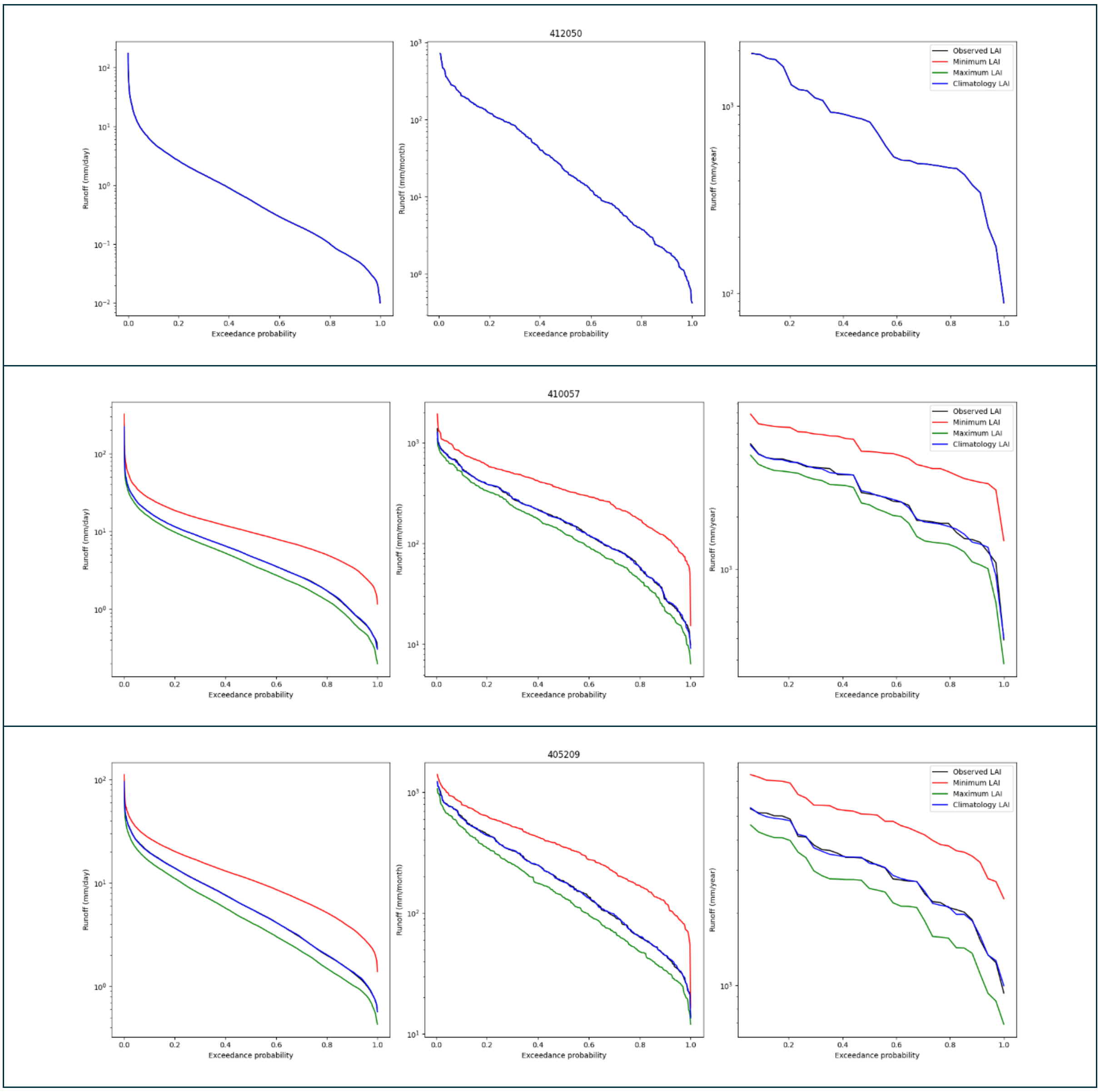

Figure 5 Sensitivity of daily, monthly and annual flow-duration curves to LAI.

We also assess the sensitivity of the hydrological simulations to LAI by comparing simulated annual time series generated using observed and climatology LAI (Figure 6). As expected, for the catchment where the model is not sensitive to LAI, there is no difference in the annual time series generated using the climatology and observed LAI. For the catchments that are sensitive to LAI, differences between the runoff time series generated using observed and climatology LAI exist and two different behaviours are observable. Differences between the annual runoff time series generated using observed and climatology LAI for catchment 410057 appear to be random, with runoff generated using the climatology LAI oscillating about the time series generated using observed LAI and anomalies persisting for no more than 2-3 years. Before 2008, catchment 405209 displays similar behaviour to catchment 410057, with the runoff generated using the climatology LAI oscillating about the time series generated using observed LAI. However, after 2008, runoff generated using the observed LAI is consistently higher than that generated using the climatology LAI, although the differences decrease with time after 2008. Catchment 405209 was heavily impacted by the Black Saturday bushfires of the 2008/09 fire year and simulations indicate that the runoff has increased in the years immediately following the fire.

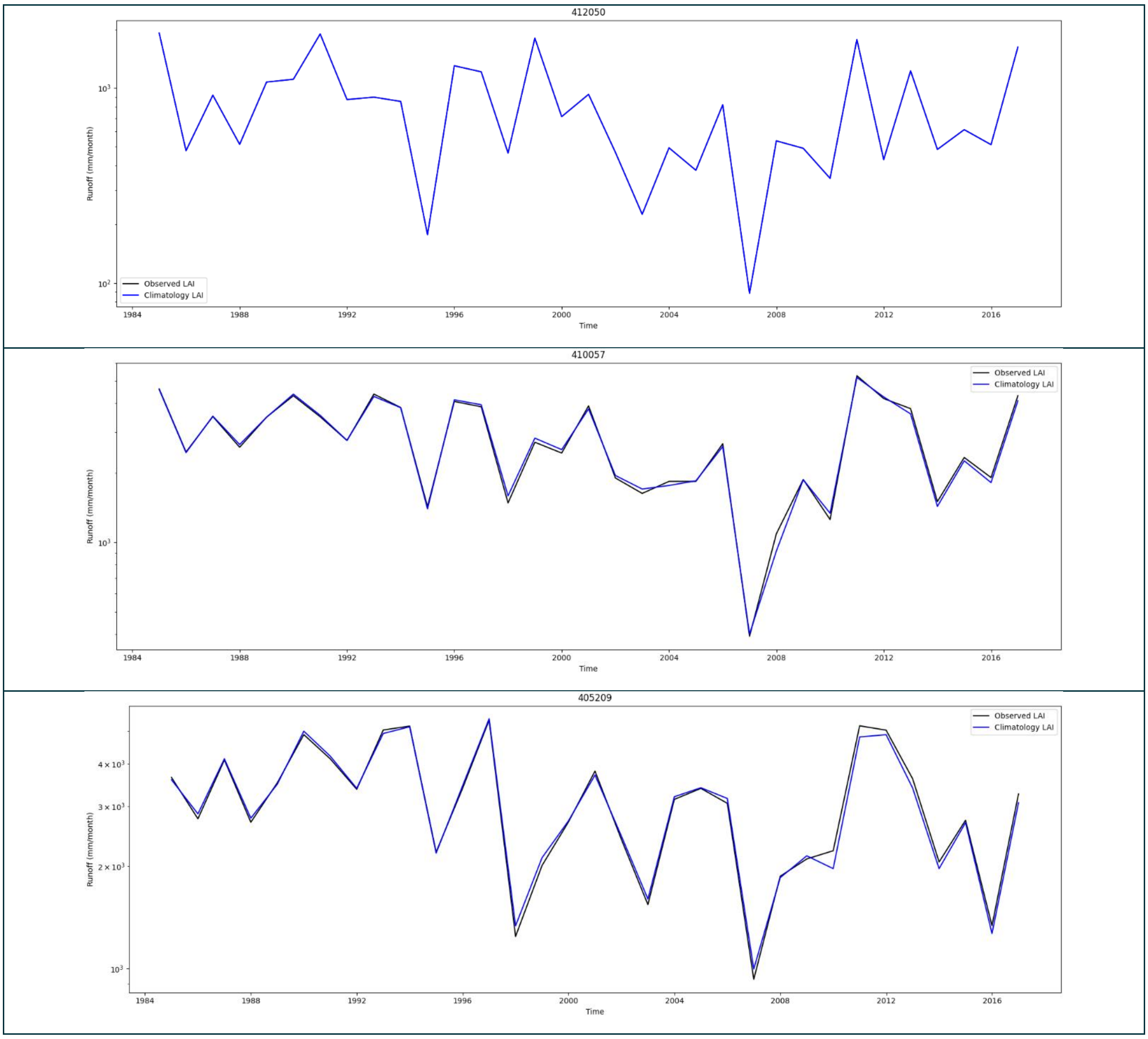

Figure 6 Example simulated time series of annual runoff for three contrasting catchments generated using observed and climatology LAI

3.2 Fire weather and occurrence

We firstly summarise the observed historical distribution of forest burn area and then evaluate the model describing the relationship between fire weather and the burnt forest area.

3.2.1 Summary of historical data

No statistically significant relationships were found between the number of days in a year exceeding the threshold for Very High (FFDI > 25), Severe (FFDI > 50) and Extreme (FFDI > 75) fire danger and the probability of fire in a catchment (Figure 7). However, a significant relationship was found between the probability of a fire occurring in a catchment and the number of days in a year the FFDI exceed the catchment 90th percentile FFDI.

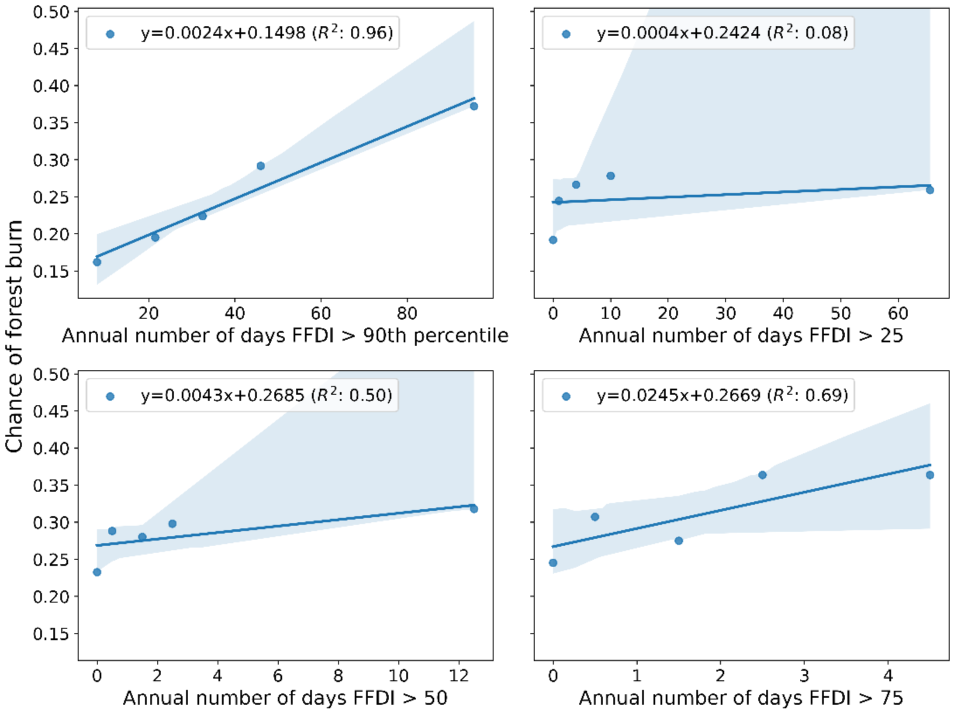

Figure 7 Relationship between the annual number of days exceeding FFDI thresholds and the probability of a fire in a forested area of the study catchments.

The number of days in a year the FFDI exceeds the catchment 90th percentile FFDI ($d_{FFDI>q90,s}$) also shows a relationship with the area of forest burnt (Figure 8). As $d_{FFDI>q90,s}$ increases, we see that the chance of a fire occurring increases and the area of forest burnt in the study catchments also increases.

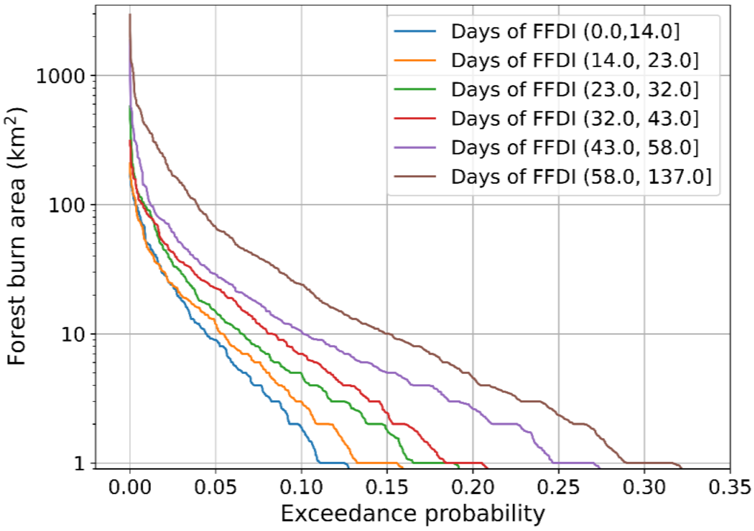

Figure 8 Distributions of observed burnt forest areas conditioned on annual FFDI days exceeding 90th percentile within the HRS catchments.

3.2.2 Modelling relating fire weather and burnt forest area

We establish a statistical model that can describe the relationship between $d_{FFDI>q90,s}$ and the distribution of forest area burnt. The model is able to characterise the shape of the probability distribution of forest burnt areas conditioned on $d_{FFDI>q90,s}$, including the probability of the forest burnt area exceeding 1 km^2, as indicated by the orange line corresponding to the empirical observations falling within the upper and lower bounds of the corresponding fitted model (Figure 9).

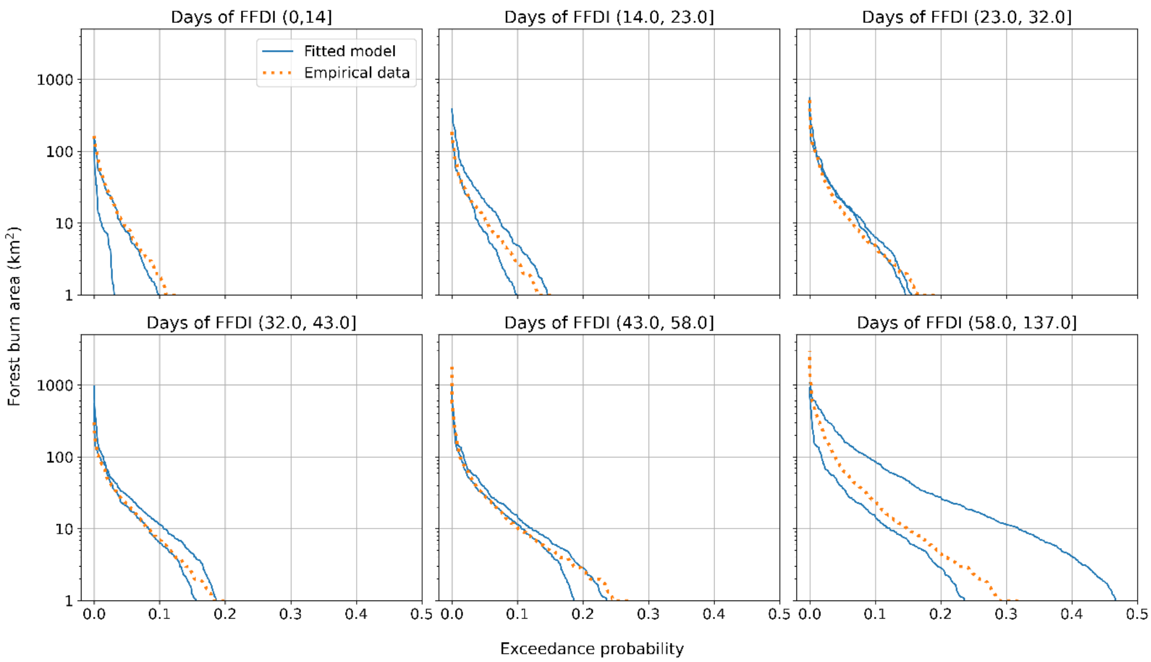

Figure 9 Comparison of fitted model relating catchment forest burnt areas to annual FFDI days exceeding 90th percentile and corresponding empirical distribution. Fitted model lines are for annual FFDI exceedance days at the upper and lower bounds of the bin used to estimate the empirical distribution.

We assess how well the fitted model represents the uncertainty in predictions of forest burn area using a probability integral transform (PIT) – uniform probability plot (Figure 10). The fitted model relating $d_{FFDI>q90,s}$ to the catchment forest burnt area appears to represent the uncertainty in predictions extremely well, with the PIT values closely following a uniform distribution, i.e. following the 1:1 line in (Figure 10). This indicates that for a given $d_{FFDI>q90,s}$ the distribution of burnt forest area generated by the fitted model describes is consistent with observations and that the model can be used for prediction.

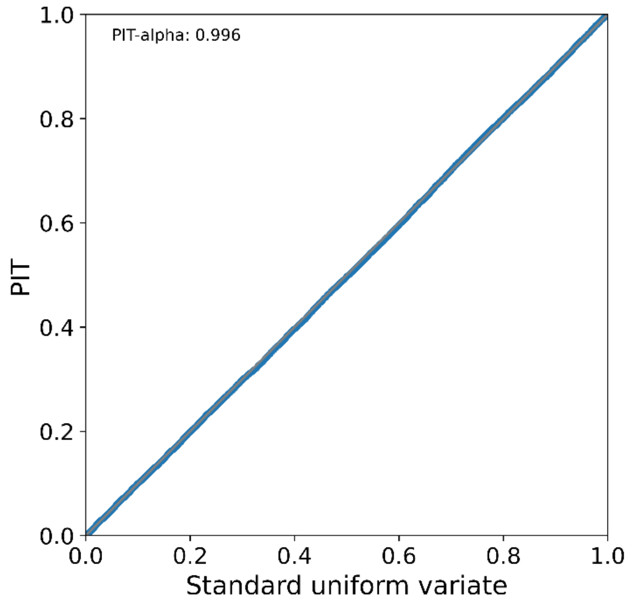

Figure 10 Probability integral transform (PIT) – uniform probability plot used to assess the ability of the fitted relationship between forest burnt area and annual FFDI days exceeding 90th percentile to adequately represent the uncertainty in forest burnt area predictions. Predictions that perfectly represent prediction uncertainty follow the 1:1 line.

The PIT-uniform probability plot assesses the uncertainty of the entire predicted distribution of forest burnt areas. We also assess the adequacy of the model to predict the probability that the forest burnt area is greater than the minimum observable area (1 km^2), using a reliability, or attributes, diagram (Figure 11). The points closely follow the 1:1 line indicating that the probability of the forest burnt area exceeding the minimum observable area is well estimated. The largest numbers of forecast probabilities fall into the range 0.1-0.3 as indicated by the largest blue circles. This suggests that for the majority of years and catchments the probability of a fire that burns at least 1 km^2 in the catchments considered is less than 0.3, but for more extreme years the probably may increase to be above 0.5. The corollary of this result presented in Figure 11 is that the probability of no forest fire $P(forest\_burnt\_area) \leq 1km^2) = (1.0 - P(forest\_burnt\_area\ ) > 1km^2)\ )$ is also well estimated.

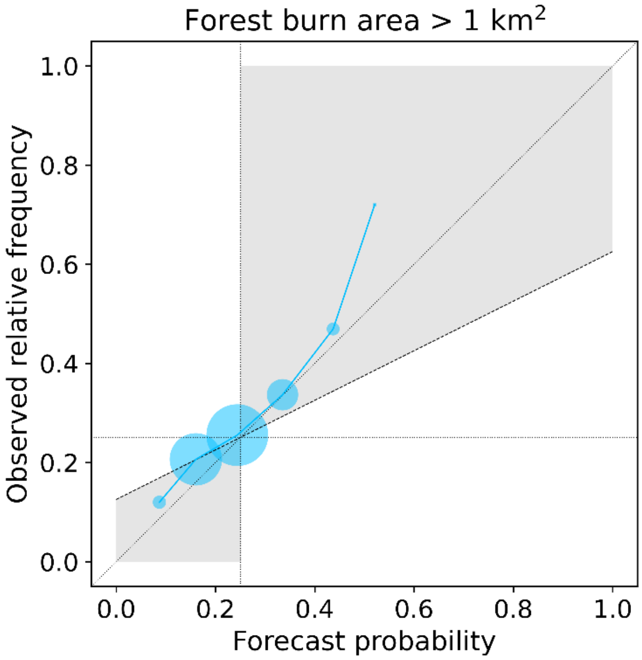

Figure 11 Reliability diagram used to assess the adequacy of the fitted relationship between forest burnt area and annual FFDI days exceeding 90th percentile to predict the probability of the burnt area exceeding 1km^2. Ideally the blue line will follow the 1:1 line. The number of events in each forecast probability bin is represented by the size of the blue circles.

3.3 Impact of fire on vegetation

3.3.1 Leaf area index changes due to fire

We firstly characterise the impact of fire on vegetation by assessing how annual changes in leaf area index are related to the occurrence of fire. In years where a fire does not occur, the annual LAI change has a mean of very close to zero and a range of approximately ±1.0 (Figure 12). This indicates that there is variability in annual LAI values, and even when no fire occurs LAI can decrease over a year. In years where a fire does occur, there is a much greater chance that the annual LAI change will be negative, that is that fire reduces the leaf area index, than when there is no fire. However, there is also a chance that the LAI will still increase over a year, which may arise due to an early-season or a low intensity fire that promotes understorey growth.

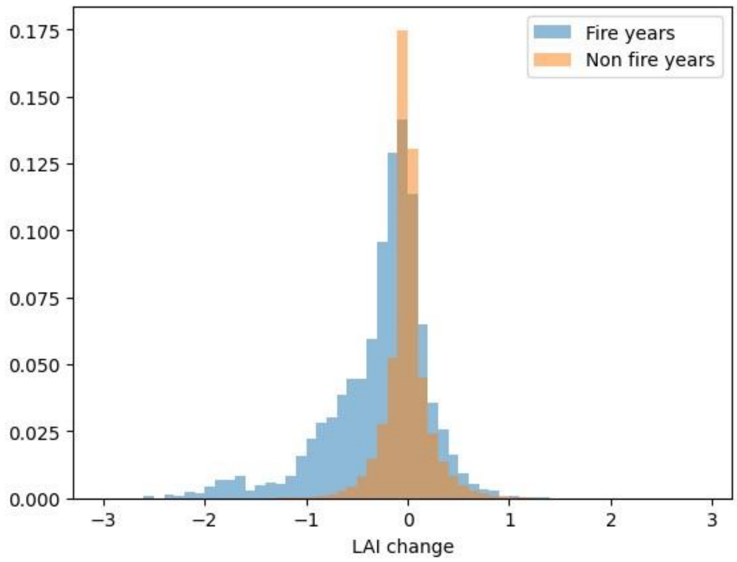

Figure 12 Normalised density of annual LAI change for fire and non-fire years.

Changes in LAI are found to be dependent on $d_{FFDI>q90,s}$ (Figure 13). During non-fire years, the dependence of LAI is weak and while the mean and median change is slightly negative for $d_{FFDI>q90,s}$ values greater than 75, the 5th percentile of the distribution is always greater than zero. A slight dependence of LAI on $d_{FFDI>q90,s}$ during non-fire years is not unexpected as years where $d_{FFDI>q90,s}$ is high are hot and dry, and vegetation will often respond by reducing exposed leaf area.

During fire years, the relationship between LAI change and $d_{FFDI>q90,s}$ is stronger than during non-fire years when $d_{FFDI>q90,s}$ is high. During the most extreme years when fires occur the mean decreases in individual 1 km pixel LAI can be as much as 1.0 with a range that extends to 2.0. However, when fires occur in years where $d_{FFDI>q90,s}$ is less than about 40 days, the change in LAI is virtually indistinguishable from non-fire years.

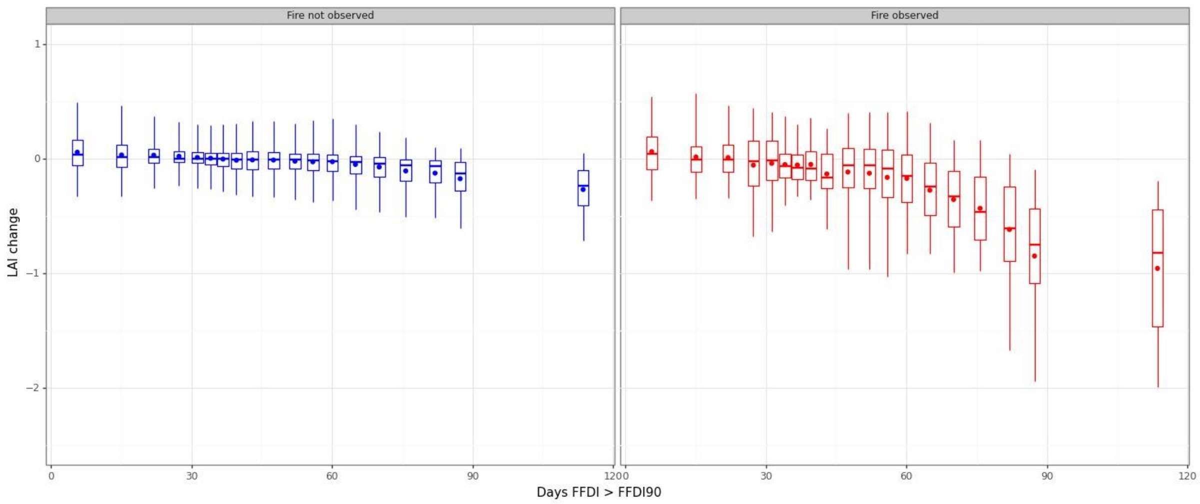

Figure 13 Annual changes in LAI for fire and non-fire years conditioned on the annual FFDI days exceeding the 90th percentile. The boxes are derived from the 25th and 75th percentiles, the whiskers extend to the 5th and 95th percentiles, and the median and mean are shown as horizontal lines and points, respectively.

To be able to predict the impact of fire on LAI we establish a piecewise regression model relating LAI change in fire years to $d_{FFDI>q90,s}$ (Figure 14). The parameters of the piecewise regression relationship, including the slopes and intercepts of the two segments and breakpoint between them, were estimated jointly by maximising the likelihood function, and thereby minimising the prediction variance. The breakpoint between the two segments was estimated to be $d_{FFDI>q90,s} \approx 50$, with a steeper slope for $d_{FFDI>q90,s}$ values larger than the breakpoint. The shaded 50th percentile prediction errors in Figure 14 closely correspond to the 50th percentile of the observations, suggesting that the model can adequately estimate the predictive uncertainty.

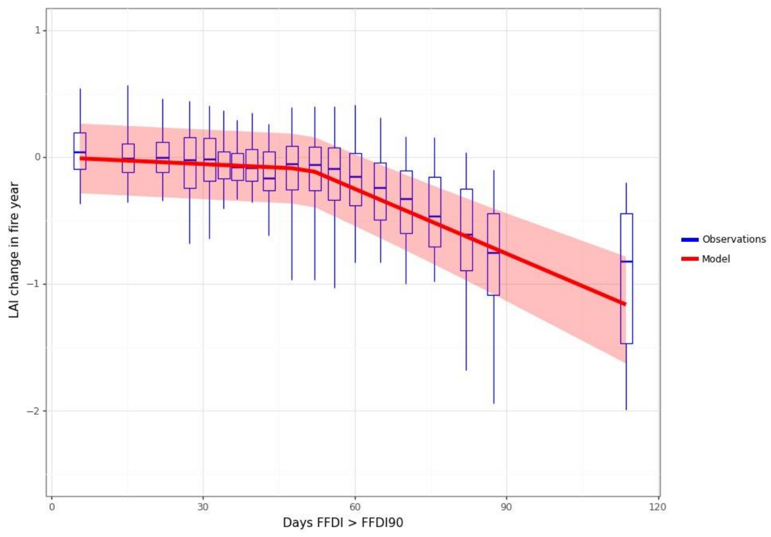

Figure 14 Modelled and observed relationship between the annual FFDI days exceeding the 90th percentile and annual LAI changes during fire years. Box plots for observations are described above, modelled mean represented by the solid red line and the 50 percentile prediction intervals by the red shading.

3.3.2 Post-fire recovery of leaf area index

Post-fire recovery of LAI was investigated by examining how the proportion of LAI fire impacts reduce with the time since a fire (Figure 15). The average observed recovery of LAI following fire shows an initial rapid recovery over the first 5 years that progressively slows over time and tends to asymptote to pre-fire LAI levels, or the proportional impact in Figure 15 approaches 1.0. There is considerable variability in the post-fire recovery of LAI between grid cells as indicated by the large range of the boxes and whiskers, but this range is commensurate with the interannual variability of LAI in non-fire years. It is also noticeable that on some occasions during the post-fire recovery the LAI can exceed the pre-fire LAI (the proportional impact in Figure 15 is greater than 1.0), which is also consistent with the considerable variability in LAI changes shown in Figure 12. We examined whether the post-fire recovery of LAI varied with vegetation type or fire severity but found no clear differences in the rate of change or variability of responses.

The fitted model characterises the general response of the observations, and the prediction intervals match the uncertainty in the observations for the majority of years since fire (Figure 15). After 10-12 years, the mean prediction is for the LAI to be at least 90% of its pre-fire level. We note that the representation of the fitted model in Figure 15 and particularly its prediction uncertainties is a conceptual representation of the actual model. The actual model is applied to LAI values and not the proportional recovery (see Equation 9).

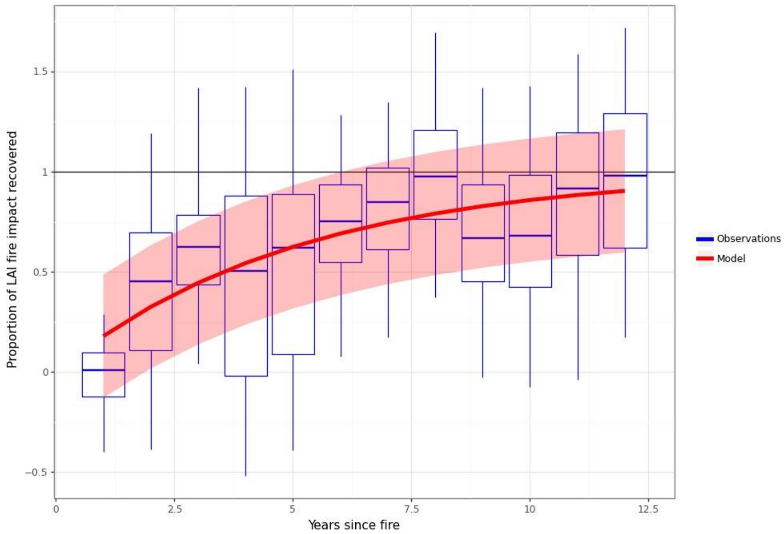

Figure 15 Modelled and observed recovery of annual LAI with time since fire. Box plots for observations are described above, modelled mean represented by the solid red line and the 50%ile prediction intervals by the red shading.

3.4 Future projections

To illustrate the future projections, we firstly provide illustrative examples for a single example catchment and then summarise results for all catchments.

3.4.1 Projections for an example catchment

We select the catchment of the Goobarragandra River at Lacmalac (gauge 410057) to illustrate the future projections of bushfire and its impacts on runoff under a climate change scenarios. The Goobarragandra catchment is a tributary of the Tumut and Murrumbidgee rivers with an area of 667 km^2, of which 83% is forested. For a projected 2°C increase in temperature and 10% decline in rainfall, the fire weather index $d_{FFDI>q90,s}$ increases by approximately 20 days per year for approximately 75% of years and somewhat less than that for the remaining 25% of years (Figure 16).

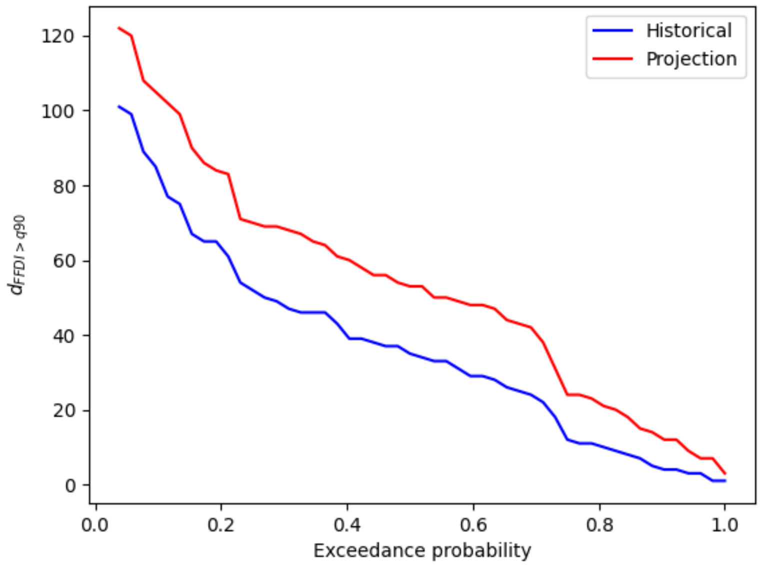

Figure 16 Exceedance curves for historical and projected $d_{FFDI>q90,s}$ for the Goobarragandra River at Lacmalac (Gauge 410057).

Using the statistical model that relates the burnt forest area to $d_{FFDI>q90,s}$, the modelled burnt forest area is predicted to increase under the future climate scenario (Figure 17). The median probability of fire occurrence (> 1 km^2 burnt) increases from approximate 0.25 under the historical climate to approximately 0.35 under the projected future climate. However, as the forest burn area increases the changes in the exceedance probability due to future climate, changes are smaller than the change in the probability of occurrence. There is considerable overlap in the prediction uncertainties of the forest burn areas generated for the historical and projected future climates. This suggests that while the area of forest burnt is expected to increase in response to increases in $d_{FFDI>q90,s}$, the uncertainties in statistical predictions are large, compared to changes in the predictor values.

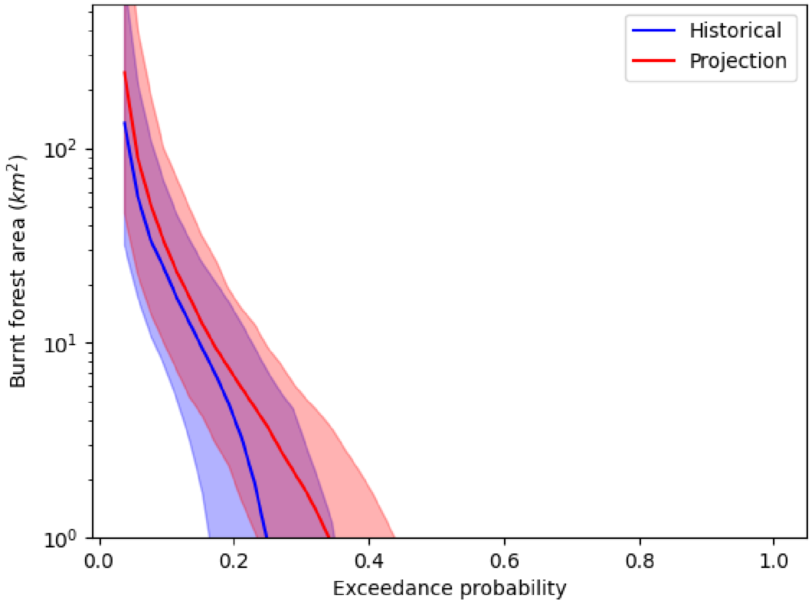

Figure 17 Exceedance curves for historical and projected burnt forest area for the Goobarragandra River at Lacmalac (Gauge 410057), solid lines represents the modelled median and the shaded range represent the 90% prediction interval (i.e. [0.05,0.95] quantile range).

The modelled median catchment average leaf area index under the projected climate is marginally lower than that under the historical climate (Figure 18). The upper extent of the prediction intervals for both historical and projected climates coincide. The lower extent of the prediction intervals for the projected climate is lower than for the historic climate, but the maximum difference is about 3.5%.

The small differences between the historical and projected model catchment average LAI can be attributed to a number of factors. Fires occur relatively infrequently (Figure 17), and typically only a small proportion of the catchment area is burnt in any fire. Impacts of fire on LAI in any year will generally occur over a small proportion of a catchment and therefore the LAI for the majority of a catchment will remain relatively unchanged. As a result, the predicted catchment average LAI may only change by a small amount for the majority of years. In the areas that are burnt, the impact of fires on LAI is variable (Figure 13) and can be unobservable if the fire weather is not severe for more than approximately 60 days per year (Figure 14). In the Goorarragandra catchment, the frequency of fire weather exceeding any high threshold approximately doubles, for example severe fire weather for more than 60 days per year occurs in approximately 20% of years during the historical period increasing to 35% of years for the projected future (Figure 16). However, the combination the partial catchment area that is impacted by fire and the potentially small impacts of fire on LAI for most of the most common fire weather conditions means that the majority of projected LAI catchment average LAI time series will have very similar characteristics to the historically modelled time series. For the projected catchment average LAI time series to differ from the historical one requires the relatively rare joint occurrence of large burnt areas and large impacts of fire on LAI.

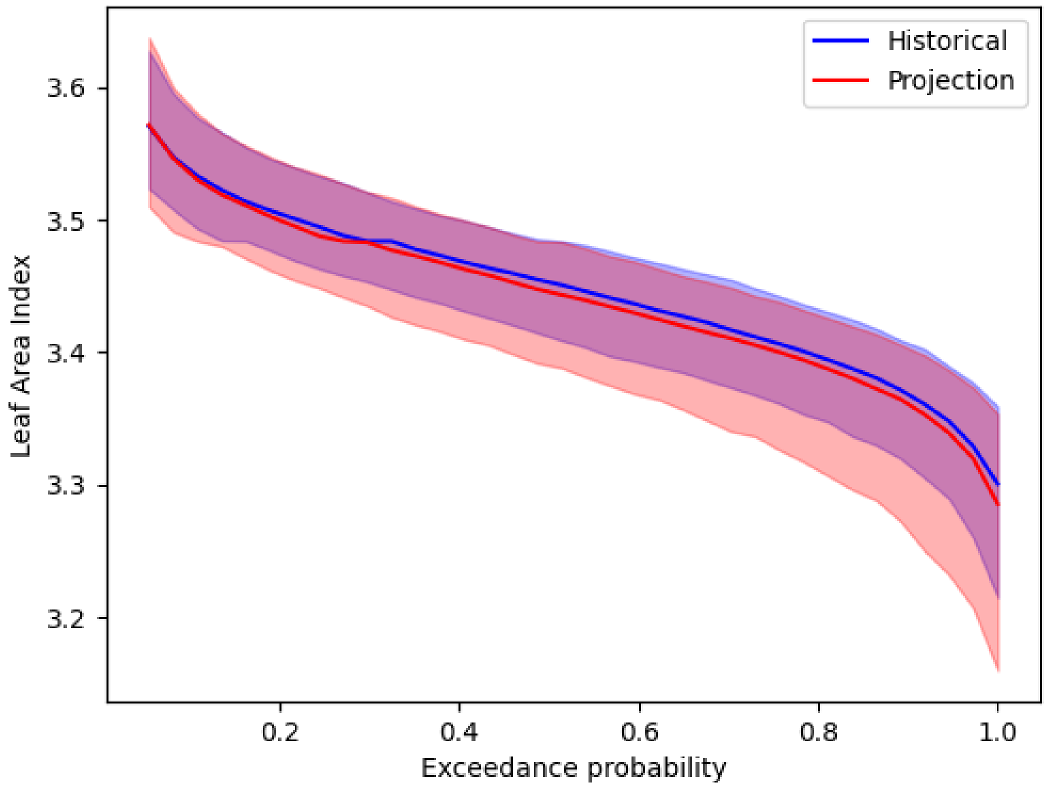

Figure 18 Exceedance curves for historical and projected catchment average Leaf Area Index for the Goobarragandra River at Lacmalac (Gauge 410057), solid lines represent the modelled median and the shaded range represent the 90% prediction interval (i.e. [0.05,0.95] quantile range).

For the Goobarragandra catchment, the impact of climate change on projected annual catchment runoff metrics is overwhelmingly dominated by projected changes in rainfall and potential evaporation. The effects of fires on the catchment runoff metrics can be observed through the quantile ranges of the metrics, which tend to be very narrow across the range. For this catchment, a 10% decrease in mean annual rainfall and 7% increase in potential evaporation leads to a decrease in all annual runoff metrics of 20-30% across the entire range of values and a similar increase in the number of days below the historical median flow.

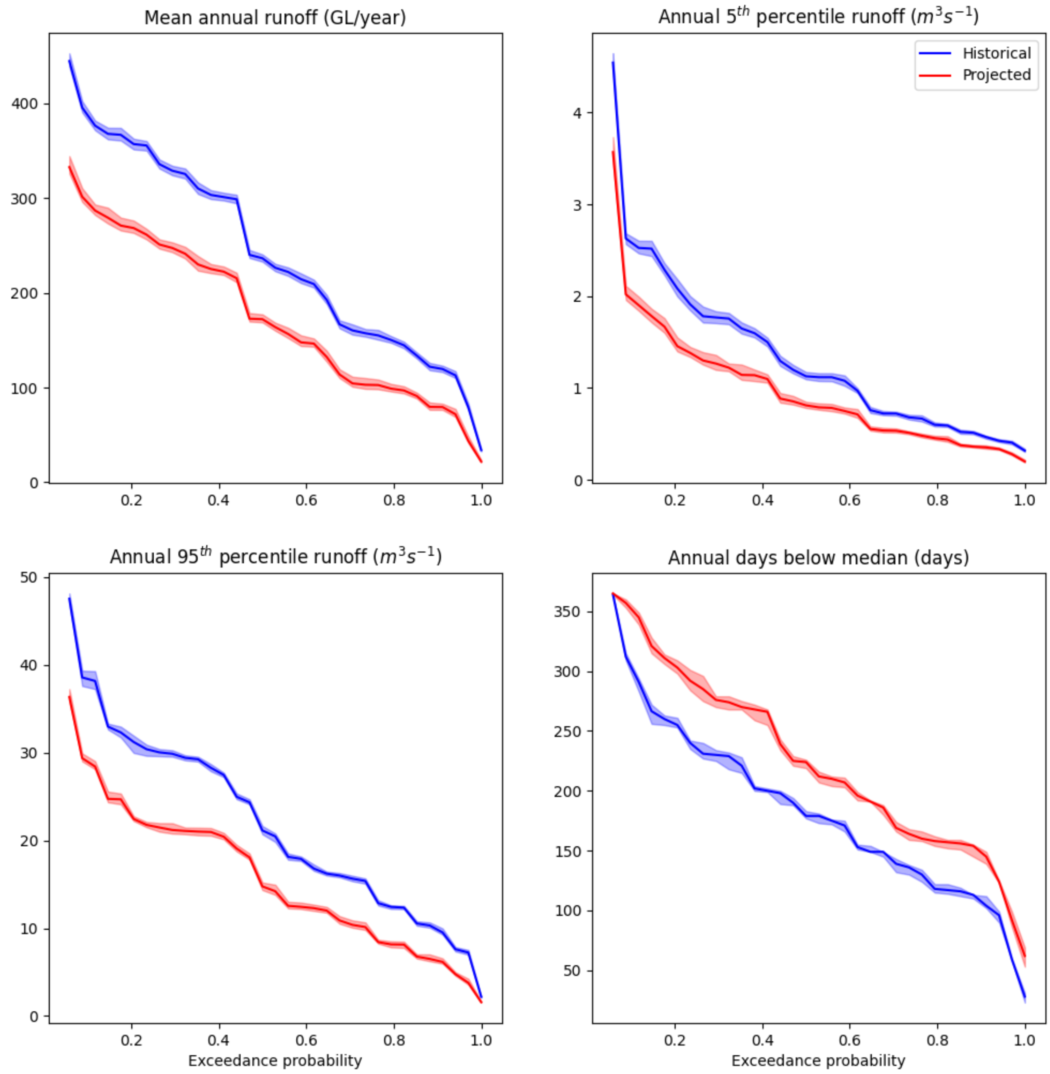

Figure 19 Exceedance curves for historical and projected simulated catchment runoff annual metrics for the Goobarragandra River at Lacmalac (Gauge 410057), solid lines represent the modelled median and the shaded range represent the 90% prediction interval (i.e. [0.05,0.95] quantile range).

3.4.2 Summary of projections for all catchments

Here we provide an overview of projections for all catchments investigated, showing changes in the occurrence of severe fire weather, catchment burn areas, LAI and runoff.

Changes in fire weather

Under a projected future climate that has 10% less rainfall, is 2°C warmer and has 7% greater potential evaporation the average $d_{FFDI>q90,s}$ increases across all HRS catchments with a median increase of approximately 24 days (Figure 20), a median increase of 65%. Increases in average $d_{FFDI>q90,s}$ vary considerably across the catchments with the greatest increases exceeding an additional 50 days in the most extreme case and the smallest increase of approximately 16 days.

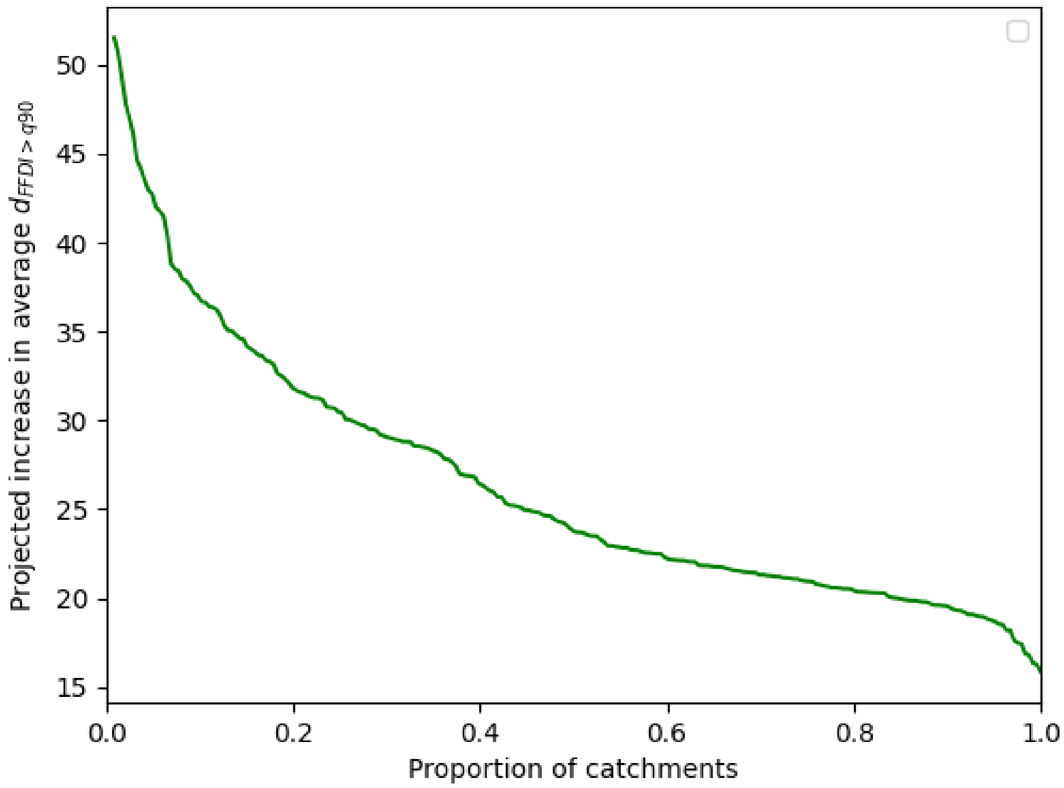

Figure 20 Summary of increases in average $d_{FFDI>q90,s}$ (days) under the projected future climate for all HRS catchments.

Changes in catchment burn area

For all catchments the projected average annual burn area is expected to increase. The mean projected increase in catchment burn area varies between 7 and 25 km^2 across the catchments investigated, equivalent to average increases of 64-280%. For each catchment, however, there are considerable differences in the average burn area across the 1000 sampled time series. For the catchment that has a mean projected increase of 25 km^2 the 90% prediction interval extends from approximately 6 km^2 to 70 km^2. This large range in projections for individual catchment stems from the uncertainty in the relationship between $d_{FFDI>q90,s}$ and the catchment burn area.

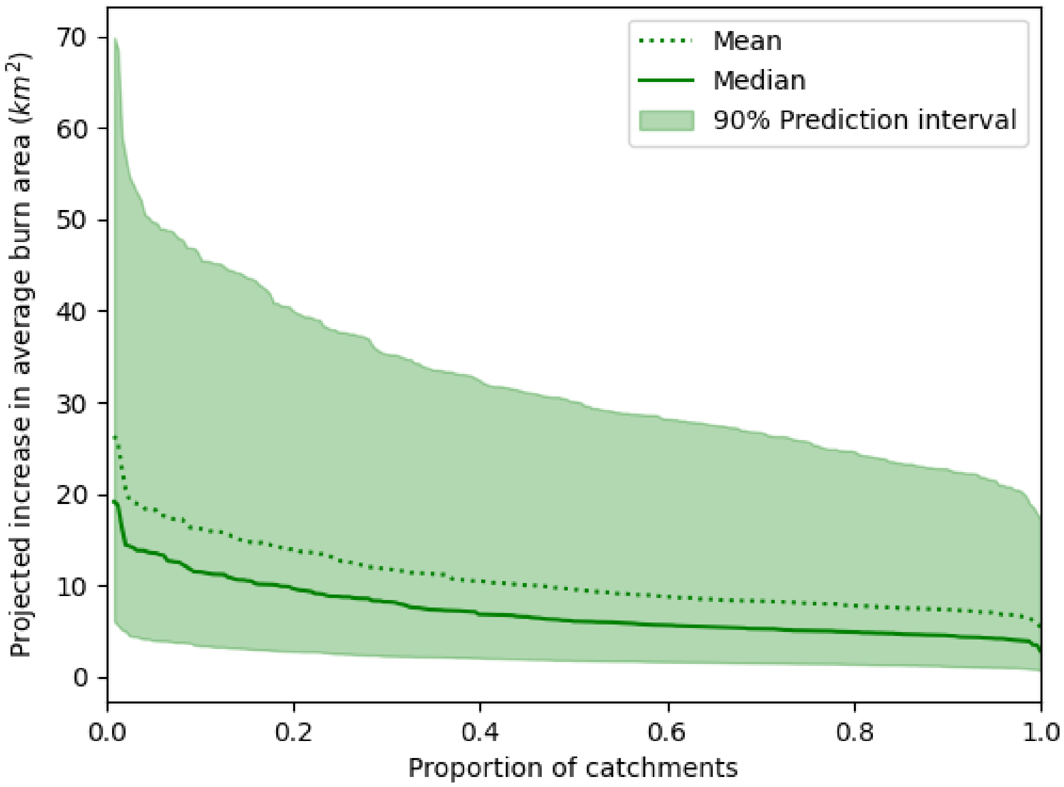

Figure 21 Summary of increases in average annual catchment burn area under the projected future climate for all HRS catchments. The pale green shading represents changes between the 90% prediction intervals of the 5th and 95th percentiles of 1000 time series generated using the modelled relationship between $d_{FFDI>q90,s}$ and catchment burn area when forced by historical and projected $d_{FFDI>q90,s}$.

Changes in leaf area index

Mean catchment average LAI is expected to decrease for almost all of the HRS catchments. The decreases in LAI tend to be relatively small (less than 0.1 m^2/m^2 or 2%) for more than 90% of catchments (Figure 22). For the catchments investigated, the largest change in the average LAI is a decrease of 0.4 m^2/m^2 (a 10% decline in average LAI), while a small number of catchments see very small increases in LAI. Changes in the mean catchment average LAI are not necessarily expected as the impacts of fire are transient, that is models will predict a recovery of LAI to a pre-fire state following a fire-induced reductions. However, if fire frequency increases to the situation where LAI doesn’t recover to the pre-fire state before the next fire occurs, then decreases in the mean catchment average LAI will be expected under climate change.

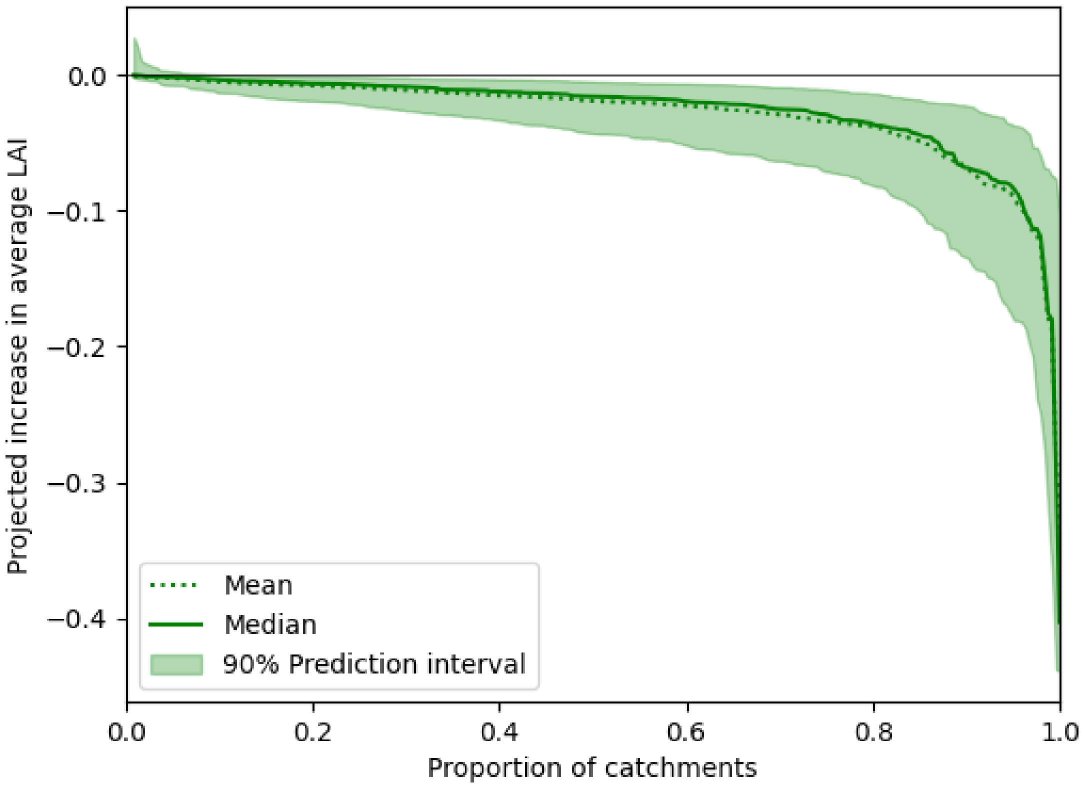

Figure 22 Summary of increases in mean catchment average LAI under the projected future climate for all HRS catchments. The pale green shading represents changes between the 90% prediction intervals of the 5th and 95th percentiles of 1000 time series.

Changes in runoff characteristics

Climate change impacts on future runoff are dominated by the direct impacts of rainfall reductions and potential evaporation increase on runoff, with bushfires having a second order effect (Figure 23). Differences between the characteristics of runoff changes simulated by the original GR4J model and the LAI-forced version are very small. The LAI-forced model which simulates the effect of bushfires on runoff, produces smaller reductions in mean annual runoff than the model that does not explicitly consider the effect of bushfires. A similar response is observed for changes in high flows, represented by the change in the mean annual 95th percentile flow. In contrast, changes in low flows, represented by the change in the mean annual 5th percentile flow, are larger for simulations from the LAI-forced model than for the model that does not explicitly consider the effects of bushfires. Differences between modelling approaches in the change in the average number of days per year that streamflow is below the historical median are very small. The results suggest that variations in LAI that are generated from projected changes in bushfire frequency, extent and severity don't necessarily have large impacts on changes in average flow characteristics. However, simulations from the LAI-forced model display larger changes in flow characteristics with smaller reductions in high flows and larger reductions in low flows compared to model that does not consider LAI. This supports the commentry of Khaledi et al. (2022), who indicated that fire is an important source of medium-term streamflow variability.

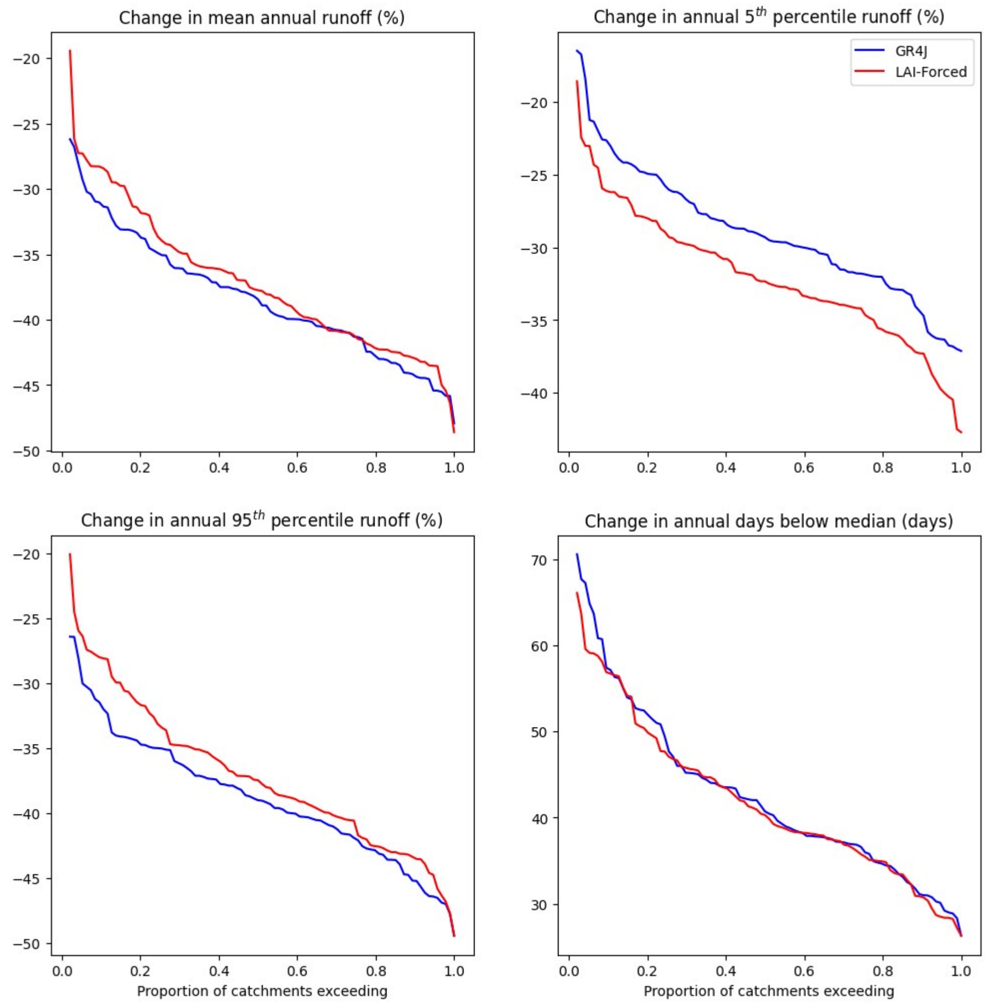

Figure 23 Summary of changes in mean annual streamflow characteristics generated using standard and LAI-forced versions of GR4J hydrological mode under the projected future climate for all HRS catchments.

We further explore changes in runoff characteristics by examining differences between modelling approaches for individual catchments and their spatial distribution. The LAI-forced version of GR4J produces smaller reductions in mean annual runoff in catchments that are predominantly located in the south-east of the MDB, while it produces larger reductions in mean annual runoff in catchments in the north of the MDB (Figure 24). The catchments where the LAI-forced version of GR4J produces much lower reductions in mean annual runoff are in the headwater catchments of the Goulburn, Murray and Murrumbidgee rivers and tend to be heavily forested. Differences in mean annual flow reductions between the modelling approaches do not appear to be related to the magnitude of the reductions in mean annual flow produced by either modelling approach.

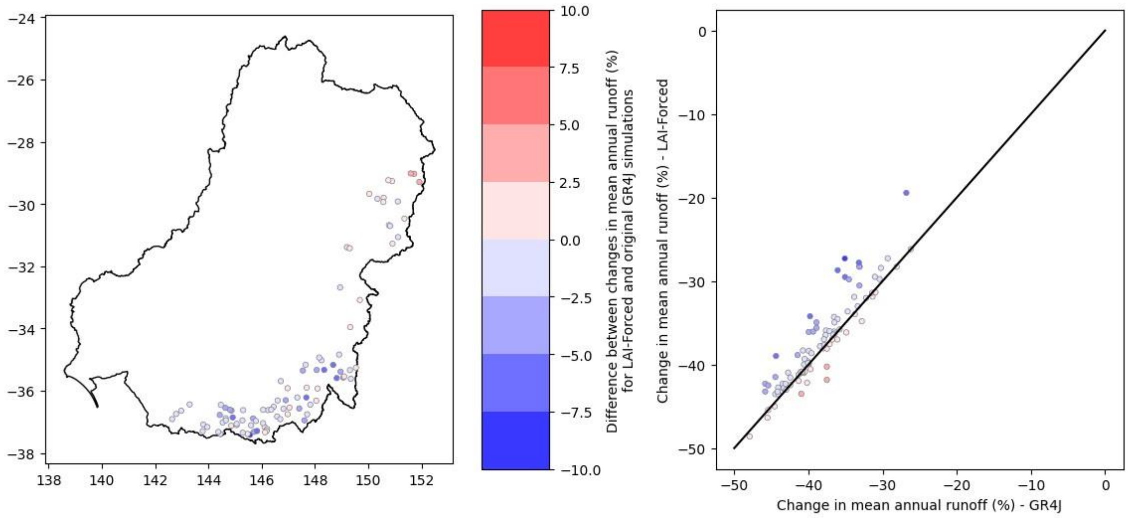

Figure 24 Differences between changes in mean annual runoff due to climate change between simulations generated using LAI-forced and original versions of the GR4J hydrological model. Negative values indicate the LAI-forced version of GR4J has smaller changes in mean annual runoff than the original version.

The LAI-forced version of GR4J produces larger reductions in low flows than the original version of GR4J for almost all catchments (Figure 25). There is no clear pattern in the location of the catchments where LAI-forced model produces the largest reductions in low flows, relative to the original version of GR4J.

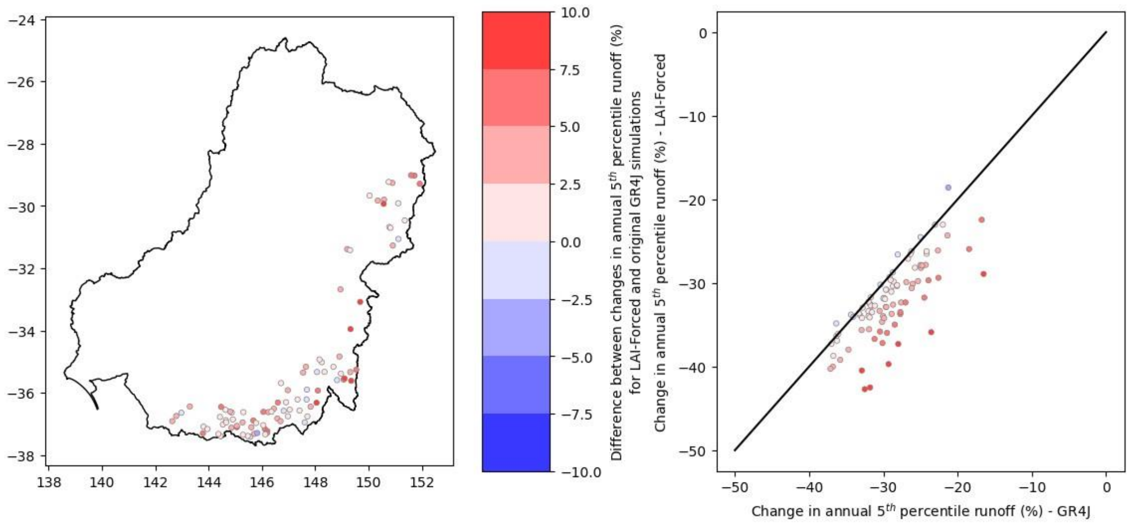

Figure 25 Differences between changes in annual 5th percentile runoff due to climate change between simulations generated using LAI-forced and original versions of the GR4J hydrological model. Negative values indicate the LAI-forced version of GR4J has smaller changes in annual 5th percentile runoff than the original version.

Finally, the spatial distribution of the catchments where the LAI-forced version produces smaller reductions in high flows, as described by the annual 95th percentile runoff, than the original version due to climate changes closely follows that of the mean annual runoff (Figure 26). The catchments where the LAI-forced version of GR4J produces much lower reductions in the annual 95th percentile flow are also located in the heavily forested headwater catchments of the Goulburn, Murray and Murrumbidgee rivers.

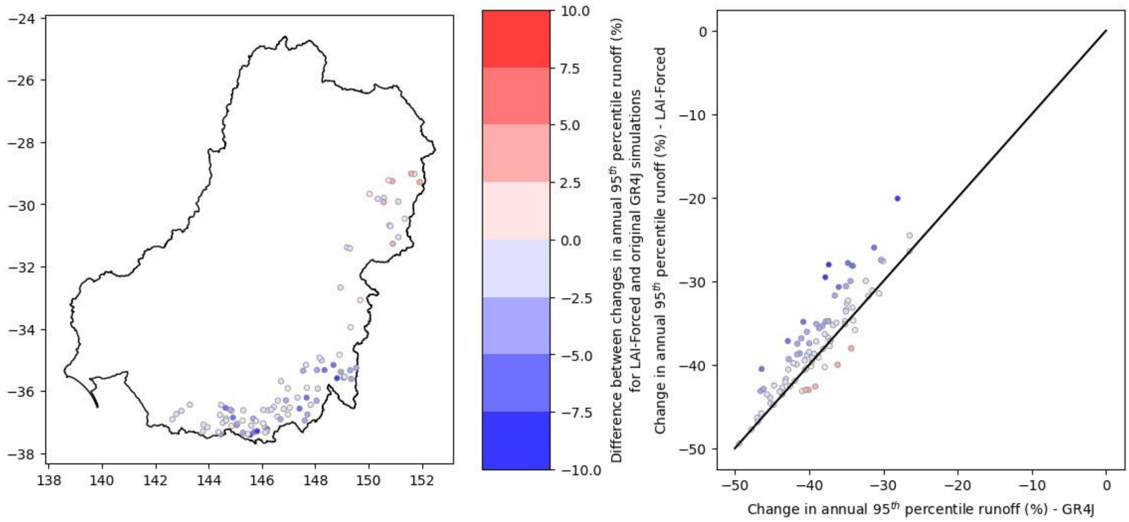

Figure 26 Differences between changes in annual 95th percentile runoff due to climate change between simulations generated using LAI-forced and original versions of the GR4J hydrological model. Negative values indicate the LAI-forced version of GR4J has smaller changes in annual 95th percentile runoff than the original version.

4 Discussion

In this study we sought to quantify the effects of climate change on catchment runoff when accounting for coincident increases in the extent and severity of bushfires and their effects on hydrological processes. Our approach has been to use historical data to relate indicators of fire weather, specifically the Forest Fire Danger Index, to (i) the forested area of catchments burnt by bushfires and (ii) the impact of bushfires on remotely sensed LAI. We have also established models that describe the recovery of LAI with time since fire, and hydrological models that are sensitive to changes in LAI. We have then used the models to estimate the impacts of climate changes, manifesting as 10% decrease in rainfall, 2°C increase in temperature and 7% increase in potential evaporation, on the burnt forest areas, catchment average LAI and subsequently catchment runoff.

Under the projected climate scenario, the average number of severe fire weather days increases by a median of 24 days per year, or 65%, (range of 15-50 days per year, or 45%-133%) across the catchments investigated, which is a relatively large increase in severe fire weather days each year. We find this leads to an increase in the average annual area of forest burnt of 10-25 km^2 (60-280% increase) for the catchments investigated. The increases in the number of severe fire weather days is amplified in the burnt forest area as the relationship the between the two appears to be non-linear. As a result of the increased forest burnt areas, the catchment average LAI is projected to decrease by less than 0.1 m^2/m^2 (2%) for more than 90% of catchments, which amounts to a relatively small decrease. Projected changes in runoff characteristics are dominated by change in rainfall and potential evaporation, with the median decline in catchment runoff of 38% (range 20%-48%) across the catchments investigated, with similar declines in high and low flow conditions.

Comparing catchment runoff projections generated using modelling that allows for the effects of bushfires to a more traditional approach that does not, we find that there are only small differences in estimates of mean annual runoff change for the majority of catchments. However, for nearly all catchments, the modelling approach that considers the effects of bushfires produces smaller reductions in the annual 95th percentile (high) runoff and larger reductions in the 5th percentile (low) runoff than the traditional modelling approach. This indicates that the annual range of runoff projections generated using the model that considers the effects of LAI is larger than the traditional approach. This result suggests that considering the effects of bushfires on catchment runoff may not necessarily be important for understanding average annual water availability under future climates. However, if daily streamflow dynamics are important for management outcomes, then modelling approaches that consider the effect of bushfires may need to be used to generate runoff projections.

Our analysis has used remotely sensed LAI data to estimate the effects of fire on vegetation, on the assumption that these data adequately represent vegetation characteristics. Multiple remotely sensed LAI datasets are available (Fang et al., 2019), and any could have been adopted for our analysis. Our choice to adopt the Zhu et al. (2013) dataset was based on a number of factors, including the length of record, spatial resolution and an assessment of data quality. To assess the data quality, we compared LAI spatial and temporal patterns with independent data. For the spatial assessment, we compare annual changes in LAI to known mapped burnt areas, finding consistent decreases in LAI over areas known to have been burnt. For a small set of locations where fires were known to have occurred and had observable impacts on vegetation, we also compared the LAI timeseries to timeseries of the remotely sensed Digital Earth Australia Fractional Cover (https://data.dea.ga.gov.au/?prefix=derivative/ga_ls_fc_3/) (Flood, 2014) to assess consistency in the time series dynamics, and in particular vegetation responses fires.

However, there are known limitations of remotely sensed LAI data that can contribute uncertainties to our analysis (Fang et al., 2019; Xu et al., 2020). One limitation relates to systematic biases in the magnitude of LAI estimates. Zhu et al. (2013) demonstrate that their LAI product has little bias, when compared to a limited number of field measurements of LAI. However, while their data are highly correlated to an alternative remote sensing derived LAI product the magnitude of values are consistently higher (Zhu et al., 2013). While these biases could introduce uncertainties into our analysis, our approach in establishing the impact of fire on LAI and also the impact of LAI on surface water hydrology, through modulation of actual evaporation, minimises the impacts of systematic errors in LAI observations by considering only relative changes in LAI. This means that our modelling approaches are influenced only by LAI change dynamics and are not impacted by errors in the magnitude of LAI values.

Impact of fire on vegetation and LAI is complex. How an individual fire behaves depends heavily on the vegetation type, site conditions (such a topography, elevation, aspect and slope), fuel loads and weather conditions, both antecedent and prevailing (Cheney, 1981; McArthur, 1967; Noble et al., 1980). The impacts of fires on vegetation and LAI are also dependent on whether the fire remains in the surface litter or reaches the forest crown (Cheney, 1981). Across a region or catchment, a diverse range of fire behaviours can occur in a single fire event and therefore impacts on LAI can also be diverse. Remotely sensed LAI observations used in this study integrate across relatively large areas, 1/12° grid cells in our analysis, and therefore some of the variability in the impact of fire on vegetation will be reduced through the averaging process. Our analysis showed a relationship between weather conditions (as characterised by the FFDI) and the magnitude of annual LAI changes resulting from fires, across our entire analysis domain, but there is considerable predictive uncertainty. One way to reduce the predictive uncertainty may be to investigate how the relationship between weather conditions and annual LAI changes can be modulated by vegetation, fuel loads or site conditions. Future investigation may be directed towards obtaining more refined estimates of the impact of fire on LAI, however the benefits may be limited by the coarse spatial resolution of remotely sensed data relative to spatial variations in the potential modulating factors.

The approach we adopted to modelling the recovery of LAI following fire is consistent with many existing models of the recovery of fire fuel (such as leaf litter) following a fire (Gould and Gomes Da Cruz, 2012). There are several variations to the form of the models for recovery of fire fuel, and the adopted model was informed by analysis of the remotely sensed LAI data. The adopted LAI recovery model asymptotically approaches the pre-fire LAI levels as the number of years after a fire increases, and the mean prediction does not exceed the pre-fire LAI. As actual evaporation is related to LAI, immediately following a fire actual evaporation will be lower that pre-fire levels and it will return and not exceed pre-fire levels. Consequently, to maintain a water balance, catchment runoff will initially increase (due to lower actual evaporation) and then decrease back to pre-fire levels over time.

The adopted LAI recovery model differs from that developed for Melbourne water supply catchments (Peel et al., 2000; Vertessy et al., 2001) and subsequently adapted for assessments of the impacts of fire in the Murray-Darling Basin (Hill et al., 2008; Mannik et al., 2013). The LAI recovery model used in these earlier studies sees the post-fire LAI exceeding the pre-fire levels for a period before asymptotically returning to pre-fire levels. The consequence of the post-fire LAI exceeding pre-fire LAI for a period is that during this period actual evaporation will also exceed pre-fire actual evaporation and, to maintain a catchment water balance, result in commensurate reductions in catchment runoff. This behaviour led to the development of the Kuczera curve that predicts catchment runoff will decline for extended periods following a fire (Kuczera, 1987). Recent empirical analysis suggests that the Kuczera curve response is not observable in many streamflow records (Khaledi et al., 2022) and runoff responses are closer to those predicted using our adopted model.

The choice of the model of LAI recovery following fire and its fitting was based on all forested grid cells and time steps for which the pre-fire LAI was known. In the process of choosing the form of the LAI recovery model, analysis was conditioned on the recovery of LAI with years since fire on vegetation type (using the 33 different vegetation types of the Land Cover data), pre-fire LAI, and the magnitude of fire impacts on LAI. The recovery of LAI following fire did not appear to differ under any of the conditioning factors, so a single LAI recovery model was adopted. The lack of clear differences in the LAI recovery following fire between the conditioning factors may reflect reality, however it may also be related to the relatively coarse spatial resolution of the LAI data averaging over higher resolution variations in the conditioning factors. Using higher spatial resolution LAI data may allow for conditional variations in LAI recovery to be better understood, but analysis periods are constrained by shorter record lengths.

Our hydrological modelling has incorporated the effects of LAI by modulating actual evaporation. The conversion of potential evaporation to actual is influenced independently by LAI and soil moisture availability. In the first step LAI influences the constrains on the total amount of water that plants can evaporate, while the soil moisture places a second constraint that is related to the water available to evaporate. This form of relationship is consistent with many other modelling tools, including simple water balance models (Allen et al., 1998) and more complex regional scale hydrological simulation models such as SWAT (Arnold et al., 1998; Gassman et al., 2007). We also investigated an alternative approach to convert potential evaporation to actual that explicitly considered interactions between LAI and soil moisture availability (not shown here). Considering these interactions did not have any substantial impact on either the hydrological model performance or future projections.

The approach taken to modulate actual evaporation using LAI results in a positive relationship between LAI and actual evaporation (Sato et al., 2008; 近藤, 1998) and therefore a negative relationship between LAI and runoff, i.e. higher LAI produces lower runoff. Preliminary statistical analysis of the relationship between LAI and catchment runoff (not shown) suggests this is the most commonly observed behaviour across the catchments investigated in this study. However, there are also several, mainly water limited, catchments that display a positive relationship between LAI and runoff, which can be attributed to both runoff and plant growth being limited by precipitation.

Our modelling of the impacts of fire on catchment runoff has focussed on medium- to long-term responses of hydrological processes as our investigation was primarily interested in water availability. Fire can also have a wide range of acute impacts on surface water hydrology that persist for a relatively short time following a fire. These acute impacts include soil surface sealing, increased erosion, and degradation of water quality as fire debris is washed into waterways and downstream storages. These acute impacts of fire can have significant consequences for water supply management immediately following a fire that, based on our results here, is likely to be greater than any long-term impacts on water resource availability.

Finally, in our modelling of the impacts of fire on catchment runoff, models of LAI recovery following fire assume that under historical and projected climates the LAI will asymptotically return to pre-fire levels, and implicitly that vegetation communities are unlikely to change. In the future, climate changes and the consequential impacts of these, such as changes to the frequency or intensity of fires, may induce change in the distribution and composition of vegetation communities. In such an eventuality, our assumption relating to post-fire LAI recovery may be inadequate. Dynamic ecosystem models are currently being developed to model the impacts of climate and fire regime changes on vegetation communities (Richards et al., 2022). The use of these dynamic ecosystem models, when available, for assessing the impacts of climate change and fire on vegetation communities and hydrological process is likely to provide a more robust assessment of climate change impacts.

5 Conclusions

Climate change is projected to increase the frequency and intensity of bushfires. Bushfires have traditionally been understood to have impacts on long-term water availability and therefore the effects of climate change on bushfires may be expected to amplify the direct impacts of climate change on catchment runoff. In this study we have assessed the potential impacts of bushfires on water availability in 245 HRS catchments in south-east Australia including more than 100 catchments in the Murray-Darling Basin. To assess the impact of bushfires on future water availability we established modelling methods that related climate forcing to fire weather, burnt areas, changes in leaf area index due to fire and its post-fire recovery, and finally adapted existing hydrological models to make them responsive to changes in LAI. Using a range of readily available datasets we calibrate and demonstrate the performance of each of the models, and also examine the sensitivity of the hydrological modelling to LAI changes. We then use the modelling chain to assess changes in catchment runoff characteristics resulting from a hotter and drier future climate, characterised by a 10% decline in rainfall and 2°C increase in temperature, leading to a 7% increase in potential evaporation, relative to the historical climate, and compare these changes to those obtained using a more traditional modelling methods that do not consider the effects of bushfires.

We find that our methods for predicting burnt forest areas from fire weather, changes in LAI due to fire and the recovery of LAI following fire represent historically observed data and provide robust quantification of prediction uncertainties. We also find that the performance of the adapted hydrological model that is responsive to LAI changes is equal to or slightly better than the unadapted model for out-of-sample runoff predictions.

Under the investigated future climate scenario, we find that the fire weather is projected to be more severe, and frequency and extent of bushfires is projected to increase. Catchment average LAI is projected to decrease due to the increased frequency and extent of bushfires, but the reductions are relatively small because fires are still expected to occur relatively infrequently and any individual fire will only cover part of the catchment. Changes in future runoff are expected to be dominated by the direct impacts of changes in future rainfall and potential evaporation. Including the effects of bushfires in modelling the runoff response to climate change had little impact on mean annual runoff for the majority of catchments investigated, while for a small number of catchments changes in mean annual runoff were smaller when the effects of bushfires were included in modelling. While modelled changes in mean annual runoff were generally insensitive to the effects of bushfires, high and low flow conditions were observed to be sensitive with smaller reductions in high flow conditions and larger reductions in low flow conditions when the effects of bushfires are represented in hydrological modelling. These results indicate that using traditional hydrological modelling that does not explicitly consider the effects of bushfires for climate change projections will provide robust estimates of changes in mean annual flow, however if future changes in daily streamflow variability are important for management, then the effects of bushfires may need to be considered.

6 References

Allen, R.G., Pereira, L.S., Raes, D., Smith, M., 1998. Crop Evapotranspiration - Guidelines for Computing Crop Water Requirements. FAO, Rome, 1-326 pp.

Arnold, J.G., Srinivasan, R., Muttiah, R.S., Williams, J.R., 1998. Large area hydrologic modeling and assessment part I: Model development. JAWRA Journal of the American Water Resources Association, 34(1): 73-89. DOI:https://doi.org/10.1111/j.1752-1688.1998.tb05961.x

Benyon, R. et al., 2010. Comment on Wood et al. 2008, 'Impacts of fire on forest age and runoff in mountain ash forests'. Functional Plant Biology, 37(12): 1187-1191. DOI:https://doi.org/10.1071/FP10141

Benyon, R.G., Inbar, A., Sheridan, G.J., Lyell, C.S., Lane, P.N.J., 2023. Variable self-thinning explains hydrological responses to stand replacement in even-aged forests. Journal of Hydrology, 618: 129157. DOI:https://doi.org/10.1016/j.jhydrol.2023.129157

Boyer, E.W., Wagenbrenner, J.W., Zhang, L., 2022. Wildfire and hydrological processes. Hydrological Processes, 36(7): e14640. DOI:https://doi.org/10.1002/hyp.14640

Brown, J.A.H., 1972. Hydrologic effects of a bushfire in a catchment in south-eastern New South Wales. Journal of Hydrology, 15(1): 77-96. DOI:https://doi.org/10.1016/0022-1694(72)90077-7

Canadell, J.G. et al., 2021. Multi-decadal increase of forest burned area in Australia is linked to climate change. Nature Communications, 12(1): 6921. DOI:10.1038/s41467-021-27225-4

Charles, S.P. et al., 2020. Impact of downscaled rainfall biases on projected runoff changes. Hydrol. Earth Syst. Sci., 24(6): 2981-2997. DOI:10.5194/hess-24-2981-2020

Cheney, N.P., 1981. Fire Behaviour. In: Gill, A.M., Groves, R.H., Noble, I.R. (Eds.), Fire and the Australian Biota. Australian Academy of Science, Canberra, pp. 151-176.

Chiew, F. et al., 2008. Rainfall-runoff modelling across the Murray-Darling Basin, CSIRO, Australia. DOI: https://doi.org/10.4225/08/585ac5cb01c1e

Chiew, F. et al., 2017. Future runoff projections for Australia and science challenges in producing next generation projections, MODSIM. MSSANZ, Hobart, pp. 1745-1751.

Chiew, F.H.S., Zheng, H., Potter, N.J., 2018. Rainfall-Runoff Modelling Considerations to Predict Streamflow Characteristics in Ungauged Catchments and under Climate Change. Water, 10(10): 1319.

Dowdy, A.J., 2020. Seamless climate change projections and seasonal predictions for bushfires in Australia. Journal of Southern Hemisphere Earth Systems Science, 70(1): 120-138. DOI:https://doi.org/10.1071/ES20001

Duan, Q.Y., Gupta, V.K., Sorooshian, S., 1993. Shuffled complex evolution approach for effective and efficient global minimization. J Optim Theory Appl, 76(3): 501-521. DOI:10.1007/BF00939380

Fang, H., Baret, F., Plummer, S., Schaepman-Strub, G., 2019. An Overview of Global Leaf Area Index (LAI): Methods, Products, Validation, and Applications. Reviews of Geophysics, 57(3): 739-799. DOI:https://doi.org/10.1029/2018RG000608

Flood, N., 2014. Continuity of Reflectance Data between Landsat-7 ETM+ and Landsat-8 OLI, for Both Top-of-Atmosphere and Surface Reflectance: A Study in the Australian Landscape. Remote Sensing, 6(9): 7952-7970.

Frost, A.J., Ramchurn, A., Smith, A., 2018. The Australian Landscape Water Balance model (AWRA-L v6). Technical Description of the Australian Water Resources Assessment Landscape model version 6. Bureau of Meteorology Technical Report, Bureau of Meteorology (BoM), Australia.

Gassman, P., Reyes, M., Green, C., Arnold, J., 2007. The Soil and Water Assessment Tool: Historical Development, Applications, and Future Research Directions. Transactions of the ASABE, 50(4): 1211-1250. DOI:https://doi.org/10.13031/2013.23637

Gill, A.M., 1981. Adaptive responses of Australian vascular plant species to fires. In: Gill, A.M., Groves, R.H., Noble, I.R. (Eds.), Fire and the Australian Biota. Australian Academy of Sciences, Canberra, pp. 243-272.

Gould, J., Gomes Da Cruz, M., 2012. Australian fuel classification: stage II. National burning project: sub-project no. 5. DOI:https://doi.org/10.5072/83/5849a10074b76

Hersbach, H. et al., 2020. The ERA5 global reanalysis. Q. J. R. Meteorol. Soc., 146(730): 1999-2049. DOI:https://doi.org/10.1002/qj.3803

Hill, P.I. et al., 2008. Spatially explicit modelling of the hydrologic response of bushfires at the catchment scale. Australasian Journal of Water Resources, 12(3): 281-290. DOI:10.1080/13241583.2008.11465354

Jones, D.A., Wang, W., Fawcett, R., 2009. High-quality spatial climate data-sets for Australia. Aust. Meteorol. Oceanogr. J., 58(4): 233-248.

Khaledi, J., Lane, P.N.J., Nitschke, C.R., Nyman, P., 2022. Wildfire contribution to streamflow variability across Australian temperate zone. Journal of Hydrology, 609: 127728. DOI:https://doi.org/10.1016/j.jhydrol.2022.127728

Kondo, J., 1998. Dependence of Evapotranspiration on the Precipitation Amount and Leaf Area Index for Various Vegetation Surfaces. Journal of Japanese Society of Hydrology and Water Resources, 11(7 (in Japanese with English abstract)): 679-693. DOI:10.3178/jjshwr.11.679

Kuczera, G., 1987. Prediction of water yield reductions following a bushfire in ash-mixed species eucalypt forest. Journal of Hydrology, 94(3): 215-236. DOI:https://doi.org/10.1016/0022-1694(87)90054-0

Lane, P.N.J., Mackay, S.M., 2001. Streamflow response of mixed-species eucalypt forests to patch cutting and thinning treatments. Forest Ecology and Management, 143(1): 131-142. DOI:https://doi.org/10.1016/S0378-1127(00)00512-0

Langford, K.J., 1976. Change in yield of water following a bushfire in a forest of eucalyptus regnans. Journal of Hydrology, 29(1): 87-114. DOI:https://doi.org/10.1016/0022-1694(76)90007-X

Li, X.-Y. et al., 2021. Influences of forest fires on the permafrost environment: A review. Advances in Climate Change Research, 12(1): 48-65. DOI:https://doi.org/10.1016/j.accre.2021.01.001

Mannik, R.D., Herron, A., Hill, P.I., Brown, R.E., Moran, R., 2013. Estimating the Change in Streamflow Resulting from the 2003 and 2006/2007 Bushfires in Southeastern Australia. Australasian Journal of Water Resources, 16(2): 107-120. DOI:10.7158/13241583.2013.11465408

McArthur, A.G., 1967. Fire behaviour in eucalypt forests.

Nash, J.E., Sutcliffe, J.V., 1970. River flow forecasting through conceptual models part I -- A discussion of principles. Journal of Hydrology, 10(3): 282-290. DOI:10.1016/0022-1694(70)90255-6

Noble, I.R., Gill, A.M., Bary, G.A.V., 1980. McArthur's fire-danger meters expressed as equations. Australian Journal of Ecology, 5(2): 201-203. DOI:https://doi.org/10.1111/j.1442-9993.1980.tb01243.x

Paul, M.J. et al., 2022. Wildfire Induces Changes in Receiving Waters: A Review With Considerations for Water Quality Management. Water Resources Research, 58(9): e2021WR030699. DOI:https://doi.org/10.1029/2021WR030699

Peel, M. et al., 2000. Predicting the water yield impacts of forest disturbance in the Maroondah and Thomson catchments using the Macaque model. Rep. 00/14, CRC for Catch. Hydrol., Vic., Australia.

Perrin, C., Michel, C., Andreassian, V., 2003. Improvement of a parsimonious model for streamflow simulation. Journal of Hydrology, 279(1-4): 275-289. DOI:10.1016/s0022-1694(03)00225-7

Prosser, I.P., Chiew, F.H.S., Stafford Smith, M., 2021. Adapting Water Management to Climate Change in the Murray–Darling Basin, Australia. Water, 13(18): 2504.

Richards, A. et al., 2022. A cloud-based dynamic ecosystem modelling platform for bushfire fuel prediction: System requirements and implementation plan.

Sato, Y. et al., 2008. Analysis of long-term water balance in the source area of the Yellow River basin. Hydrological Processes, 22(11): 1618-1629. DOI:https://doi.org/10.1002/hyp.6730

Vertessy, R.A., Watson, F.G.R., O'Sullivan, S.K., 2001. Factors determining relations between stand age and catchment water balance in mountain ash forests. Forest Ecology and Management, 143(1): 13-26. DOI:https://doi.org/10.1016/S0378-1127(00)00501-6

Viney, N. et al., 2009. The usefulness of bias constraints in model calibration for regionalisation to ungauged catchments. In: Anderssen, R., et al. (Eds.), 18th IMACS World Congress - MODSIM09 International Congress on Modelling and Simulation, pp. 3421-3427.

Wang, Q.J., Robertson, D.E., 2011. Multisite probabilistic forecasting of seasonal flows for streams with zero value occurrences. Water Resources Research, 47(2). DOI:http://dx.doi.org/10.1029/2010WR009333

Wang, Q.J., Robertson, D.E., Chiew, F.H.S., 2009. A Bayesian joint probability modeling approach for seasonal forecasting of streamflows at multiple sites. Water Resources Research, 45. DOI:10.1029/2008WR007355

Xu, J., Quackenbush, L.J., Volk, T.A., Im, J., 2020. Forest and Crop Leaf Area Index Estimation Using Remote Sensing: Research Trends and Future Directions. Remote Sensing, 12(18): 2934.

Zhang, Y. et al., 2013. Collation of Australian modeller's streamflow dataset for 780 unregulated Australian catchments. CSIRO, CSIRO, Australia.

Zhu, Z. et al., 2013. Global Data Sets of Vegetation Leaf Area Index (LAI)3g and Fraction of Photosynthetically Active Radiation (FPAR)3g Derived from Global Inventory Modeling and Mapping Studies (GIMMS) Normalized Difference Vegetation Index (NDVI3g) for the Period 1981 to 2011. Remote Sensing, 5(2): 927-948.

近藤, 純., 1998. 種々の植生地における蒸発散量の降水量および葉面積指数への依存性. 水文・水資源学会誌, 11(7): 679-693. DOI:10.3178/jjshwr.11.679

As Australia's national science agency and innovation catalyst, CSIRO is solving the greatest challenges through innovative science and technology.

CSIRO. Unlocking a better future for everyone.

Contact us

1300 363 400
+61 3 9545 2176
csiro.au/contact
csiro.au

For further information

E**nvironment**
David Robertson
+61 0 9**545 2431**
david.robertson@csiro.au
https://www.csiro.au/en/about/people/business-units/environment